

Interaction networks in persistent Lotka-Volterra communities

Lyle Poley ¹, Tobias Galla ², and Joseph W. Baron ^{3,*}

¹*Theoretical Physics, Department of Physics and Astronomy, School of Natural Science, The University of Manchester, Manchester M13 9PL, United Kingdom*

²*Instituto de Física Interdisciplinar y Sistemas Complejos IFISC (CSIC-UIB), 07122 Palma de Mallorca, Spain*

³*Laboratoire de Physique de l'Ecole Normale Supérieure, ENS, Université PSL, CNRS, Sorbonne Université, Université de Paris, F-75005 Paris, France*



(Received 12 April 2024; revised 27 November 2024; accepted 9 December 2024; published 28 January 2025)

A central concern of community ecology is the interdependence between interaction strengths and the underlying structure of the network upon which species interact. In this work we present a solvable example of such a feedback mechanism in a generalized Lotka-Volterra dynamical system. Beginning with a community of species interacting on a network with arbitrary degree distribution, we provide an analytical framework from which properties of the eventual "surviving community" can be derived. We find that highly connected species are less likely to survive than their poorly connected counterparts, which skews the eventual degree distribution towards a preponderance of species with lower degrees. Furthermore, the average abundance of the neighbors of a species in the surviving community is lower than the community average (reminiscent of the famed friendship paradox). Finally, we show that correlations emerge between the connectivity of a species and its interactions with its neighbors. More precisely, we find that highly connected species tend to benefit from their neighbors more than their neighbors benefit from them. These correlations are not present in the initial pool of species and are a result of the dynamics.

DOI: [10.1103/PhysRevE.111.014318](https://doi.org/10.1103/PhysRevE.111.014318)

I. INTRODUCTION

The modern discipline of macroecology takes up the ambitious challenge of identifying and understanding the unifying characteristics of ecological communities. Such characteristics include the shapes of abundance distributions, fluctuations in species abundances, and abundance-diversity relationships [1–5]. Of particular interest is the relationship between ecosystem network structure and interspecies relationships [6–8]. Interaction network structure in real ecological networks has been linked to interspecies competition [9,10], stability [11–15], and the functioning of an ecosystem in the wider biosphere [16–19].

To explain some of these observed relationships, simple models have been suggested (such as the cascade and niche models), which have had success in replicating observed patterns in natural food webs [11,20–26]. The tools of statistical physics and disordered systems are particularly well suited to aiding in the study of these models, due to their emphasis on deriving universal and emergent phenomena from microscopic interactions. As such, building on the seminal work of May [27], some works have focused on how network structure can influence ecological stability by using random matrix theory [26,28–31]. However, these models simply posit the structure of the network and interaction coefficients. Therefore, it could be that the hypothesized Jacobian matrix does not correspond to any realistic ecosystem dynamics.

More recently, dynamic mean-field theory (DMFT) techniques [32,33] have been used to examine the statistics of

interactions in the surviving communities that result from plausible ecosystem dynamics [34–36]. It has been shown that intricate correlations between species' interaction coefficients arise in these so-called feasible model communities, and that these statistics are important for stability [37].

In this work, we seek to understand what kinds of interaction networks are permitted in feasible communities. We present an analytically tractable model in which an initial pool of species interacts according to generalized Lotka-Volterra dynamics. Our interest is in the long-time behavior of the community as it follows these dynamics. The degree distribution of the network on which species initially interact is an input for the model. However, because species can die out during the dynamics, the final network of surviving species is a result of the interactions, and the eventual patterns that emerge in the community are a consequence of its feasibility. In this way, our model captures some salient aspects of the feedback loop between interspecies interactions and the structure of the network on which these interactions take place. We are thus able to probe the interdependence of interaction network structure and species relationships that characterize feasible communities.

Ultimately, we are able to demonstrate several general trends (for competitive and stable communities). First, more highly connected species are less likely to survive, which skews the degree distribution towards having many species with low connectivity and few species with high connectivity (a pattern observed in natural food webs [11,23]). Second, species with higher connectivity typically have lower abundance. This in turn means that the average abundance of the neighbor of a randomly selected species is lower than

*Contact author: jwb96@bath.ac.uk

the abundance of a randomly selected species (akin to the so-called friendship paradox). Finally, we find that there are correlations between a species' connectivity and its interactions with its neighbors. On average, well-connected species will have more favorable interactions with their neighbors than their neighbors will have with them (and vice versa for poorly connected species).

The content of this work is organized as follows. In Sec. II, we describe the generalized Lotka-Volterra model and the structure of the interspecies interactions explicitly. We then outline our analytical methods for predicting the behavior of the model in the long-time limit in Sec. III, and we compare our results for the abundance distributions of species in the community to the results of numerical integration. We also analyze stability, and find that network structure can be a stabilizing influence in communities with many predator-prey and competitive interactions. In Sec. IV, we derive a simple expression for the eventual degree distribution of the community, finding that species with low degree become relatively more common, and species with high degree become relatively rare. We also examine the dynamically induced correlations that emerge between species interactions and the network, and offer biological interpretations for these correlations. We finish by discussing possible extensions to this model and the implications of our results in Sec. V. In particular, we discuss the relationship of our work to Refs. [38,39], which also analyze Lotka-Volterra dynamics with random interactions and network structure.

II. MODEL

Consider a community of N species interacting according to generalized Lotka-Volterra (GLV) dynamics. These dynamics produce feasible communities by construction (i.e., all abundances remain positive if they are so at $t = 0$). The abundance of species i at time t , written $x_i(t)$, is determined by the following set of equations:

$$\dot{x}_i(t) = x_i(t) \left[1 - x_i(t) + \sum_{j \neq i} A_{ij} \alpha_{ij} x_j(t) \right]. \quad (1)$$

We have set the intraspecific interaction coefficients to -1 , as indicated by the term $-x_i$ in the square brackets, and we chose the intrinsic growth rates equal to 1. The adjacency matrix elements $\{A_{ij}\}$ encode the structure of the network on which the species interact. The variable A_{ij} is equal to 1 if species i and j interact, and is 0 otherwise. We always impose $A_{ij} = A_{ji}$. The interaction matrix α_{ij} dictates the influence of species j on species i , provided that they interact. The values of α_{ij} for which $A_{ij} = 0$ do not play a role in the dynamics. Both the adjacency matrix \mathbf{A} and interaction matrix $\boldsymbol{\alpha}$ are random matrices. They are selected independently of each other, and are fixed throughout the dynamics.

We construct the matrix \mathbf{A} according to the random configuration model [40,41] (also known as the Chung-Lu model [42]). This generalizes the often-used Erdős-Rényi network to incorporate an arbitrary degree distribution, which we write as p_k . To generate an instance of the network, we first draw the degree of each node independently from p_k . With this degree sequence $\{k_i\}$, we set each pair (A_{ij}, A_{ji}) to one with proba-

bility $k_i k_j / (dN)$, where d is the mean degree. We set the pair to zero otherwise. For sufficiently large N , this construction will produce networks with the desired degree distribution. To ensure that the probability of connection is well defined, we require $k_i k_j < dN$ for all i, j . We note here that the theoretical results we will derive also apply to other kinds of network. In Appendix F we confirm this using the Barabási-Albert graph. The results for the Chung-Lu model can be thought of as an "annealed network approximation" [31,43] for other graphs when $k_i k_j \ll dN$.

For simplicity, we will assume that the initial degree distribution is uniform, with width $w = k_{\max} - k_{\min}$, and with average degree $d = (k_{\max} + k_{\min})/2$. In our examples, both d and w are proportional to N . In the case of the uniform degree distribution, the condition $k_i k_j < dN$ for all (i, j) is equivalent to $(w/2 + d)^2 < dN$.

To construct an instance of the interaction matrix $\boldsymbol{\alpha}$, pairs of elements $(\alpha_{ij}, \alpha_{ji})$ are drawn identically and independently from a probability distribution with the following statistics:

$$\begin{aligned} \langle \alpha_{ij} \rangle_{\alpha} &= \frac{\mu}{d}, \\ \text{Var}(\alpha_{ij})_{\alpha} &= \frac{\sigma^2}{d}, \\ \text{Cov}(\alpha_{ij}, \alpha_{ji})_{\alpha} &= \frac{\gamma \sigma^2}{d}. \end{aligned} \quad (2)$$

The statistics of the interaction matrix are scaled with the factor of $1/d$ to ensure that the ensemble-averaged interaction strength between species in the community is $\sum_{ij} \langle A_{ij} \alpha_{ij} \rangle_{A, \alpha} / N = \mu$, and similarly for the variance $\sum_{ij} \langle (A_{ij} \alpha_{ij} - \mu/N)^2 \rangle_{A, \alpha} / N = \sigma^2$, which is commonly the case in fully connected versions of the model [32,33]. Our definition of the model parameters requires $\sigma^2 > 0$ and $|\gamma| \leq 1$.

The correlation coefficient γ controls the symmetry of interactions α_{ij} and α_{ji} in the original community, with $\gamma = 1$ for symmetric interactions ($\alpha_{ij} = \alpha_{ji}$ for all $i \neq j$), and $\gamma = -1$ for antisymmetric deviations from the mean [$\alpha_{ij} - \mu/d = -(\alpha_{ji} - \mu/d)$ for all $i \neq j$]. If we were to further assume that the pairs $(\alpha_{ij}, \alpha_{ji})$ were jointly Gaussian distributed, then γ has a simple relationship to the proportion p of interactions in the community that are of predator-prey type: $\gamma = \cos(\pi p)$ [44]. Generically, γ is a decreasing function of the proportion of predator-prey-type links in the community.

III. BEHAVIOR OF THE MODEL

A. Dynamical mean-field theory and phase diagram

Depending on the model parameters (μ, σ, γ , and the degree distribution p_k), the dynamics in Eq. (1) exhibit three distinct phases. As in existing GLV models with random all-to-all interactions [32,33,45], there is a phase in which, for a fixed interaction matrix, the dynamics converge to a unique equilibrium independently of the initial abundances. Second, there is a phase in which there are multiple stable fixed points for any given interaction matrix, or the system can remain volatile indefinitely. Finally, species abundances diverge in a third phase.

The three phases are separated from one another by the onset of a linear instability and, second, by the onset of diverging

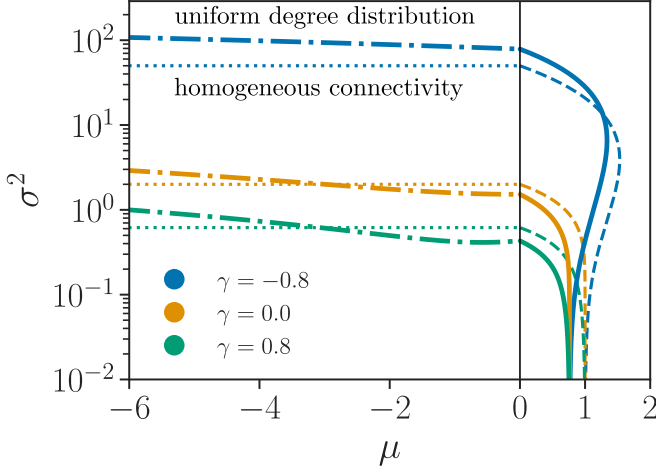


FIG. 1. Stability plot for different values of γ for the network model as described in Sec. II. The solid and dot-dashed lines show the onset of diverging abundance and of the linear instability, respectively, for uniformly distributed degrees. The dashed and dotted lines indicate diverging abundances and linear instability for the model on graphs without degree heterogeneity ($p_k = \delta_{k,d}$). Different colors represent different choices of γ as indicated in the legend. For any one model the system is stable in the area to the left of the solid or dashed curves (diverging abundance), and below the dot-dashed or dotted line (linear instability). The average degree is $d = N/4$ for all models shown. For the model with uniform degree distribution we use $w = 0.5N$. All lines in the stability plot are computed from the theory, derived in the limit $N \rightarrow \infty$.

abundances. We give an overview of our results for the phase diagram of the model in Fig. 1. As discussed in Refs. [46,47], there are other possible regimes when the interactions do not scale with the system size as above. However, we do not consider these regimes in this work.

The focus of our analytical work is on the properties of the phase in which the dynamics always converge to a unique equilibrium (independent of the initial species abundances). To this end, we employ a generating-functional method, which has its roots in the physics of disordered systems [48–51], to derive dynamical mean-field equations for the time dependence of the abundances. Dynamical mean-field theory has been successfully applied to ecological models since the work of Ref. [52] in the context of replicator equations and since the work of Ref. [32] in the context of the GLV equations.

In most previous models, the DMFT formalism produces a single effective process, which describes the dynamics of a "typical" species abundance. The statistics of this effective species mirror those of the entire community. In this work, because species in the original community are distinguishable by their degree, there is an effective process representing the typical behavior of species of each possible degree. Our treatment here follows that used to analyze a previous model in which species were distinguished not by their degree, but by their position in a hierarchy [44]. We note that our analysis, which applies most directly to the Chung-Lu model, assumes that $d \gg 1$, so that the network is not sparse. Our theory also applies to networks other than those constructed according to the Chung-Lu model, provided that $d \ll N$ (see Appendix F).

B. Characterization of the unique-equilibrium phase

In the unique-equilibrium phase, we can use the DMFT equations to find the abundance distribution of species that have a particular degree k in the original community. The derivation of the DMFT equations, as well as the analysis of the fixed point, can be found in Appendix A.

The abundance x_k^* of a typical species with degree k at the fixed point is a random variable with a clipped Gaussian distribution. The fixed-point abundances satisfy $x_k^*(z) = \max[0, x_k^{*+}(z)]$, where the nonzero abundances satisfy

$$x_k^{*+}(z) = \frac{1 + \mu \frac{k}{d} \sum_{k'} p_{k'} \frac{k'}{d} M_{k'} + z \sigma \sqrt{\frac{k}{d} \sum_{k'} p_{k'} \frac{k'}{d} q_{k'}} + h}{1 - \gamma \sigma^2 \frac{k}{d} \sum_{k'} p_{k'} \frac{k'}{d} \chi_{k'}}. \quad (3)$$

The quantity z is a zero-mean, unit-variance Gaussian random variable, and h is an external field used to define the response function χ_k below. At the end of the calculation, and in all simulations, we set $h = 0$. The quantities M_k and q_k are the first and second moments of the distribution of x_k^* , respectively. These objects are determined self-consistently from their definitions

$$\begin{aligned} M_k &= \int_{x_k^* > 0} dz f(z) x_k^*(z), \\ q_k &= \int_{x_k^* > 0} dz f(z) x_k^*(z)^2, \\ \chi_k &= \int_{x_k^* > 0} dz f(z) \frac{\partial x_k^*(z)}{\partial h}, \end{aligned} \quad (4)$$

where $f(z) = \exp(-z^2/2)/\sqrt{2\pi}$ is the probability density function of the standard normal distribution. For given model parameters, we can solve Eqs. (3) and (4) numerically to yield the values of the M_k , q_k , and χ_k , for $k = k_{\min}, \dots, k_{\max}$ (where we write k_{\min}, k_{\max} for the lowest and highest degree in the network, respectively). These quantities in turn yield the abundance distributions, i.e., the distributions for the different x_k^* . We also define the probability of survival for species that have degree k in the original community,

$$\phi_k = \int_{x_k^* > 0} dz f(z), \quad (5)$$

as well as the community-wide abundance and survival probability,

$$M = \sum_k p_k M_k, \quad \phi = \sum_k p_k \phi_k. \quad (6)$$

Figure 2 confirms the validity of the fixed-point solution from Eqs. (3) and (4). The predictions for the average abundance, survival rate, and total abundance distribution across the community match the results of simulations. We also show the prediction for the abundance distribution from a theory which does not take the full network structure into account, but instead assumes a homogenous network, where each species has the same expected degree d . That is, we set $p_k = \delta_{k,d}$, where $\delta_{k,d}$ is the Kronecker delta. As we can see from Fig. 2, the graph with homogenous expected degrees does not share the same abundance distribution as when p_k

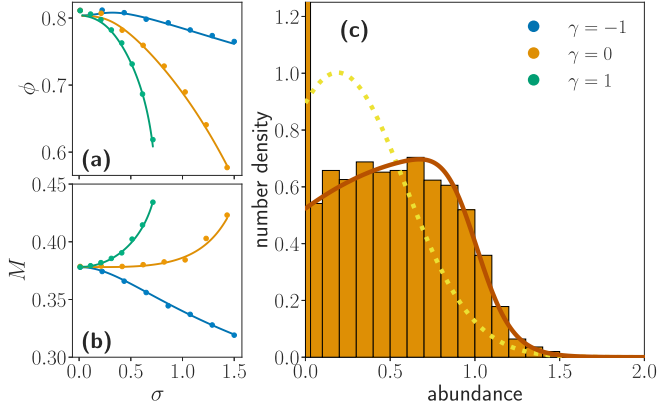


FIG. 2. (a) Overall survival probability ϕ and (b) mean abundance M in the community for varying variance of interaction strength σ . (c) The abundance distribution of species with degree k is a clipped Gaussian, and the average of all such curves gives the abundance distribution of the community as a whole (solid orange curve; see Appendix A 2 for details). The prediction from the model with network $p_k = \delta_{k,d}$ (i.e., a network with homogeneous expected degree) with the same mean, variance, correlation, and average degree d is shown as a yellow dotted curve. For all plots, the degree distribution is uniform, and the parameters are $\mu = -3$, $w = 0.45N$, and $d = N/4$ and γ is as indicated in the legend. In (a) and (b), $N = 1000$ and markers are the average over 10 runs of the dynamics. In (c), $\sigma = 1$ and $N = 5000$, and the histogram is the result of a single run of the dynamics. The large spike at zero abundance is due to species which have died.

is a uniform distribution, confirming the importance of degree heterogeneity in the theory.

C. Onset of instability

The analytical results presented in Sec. III B are only valid in the phase with a unique equilibrium. In Appendix C, we find the boundary of this stable regime in terms of the parameters of the model.

The onset of the diverging phase for given model parameters (μ , σ , γ , and p_k) is found by solving the fixed-point equations (4), together with the additional condition that the community average abundance M diverges.

To identify the point at which the dynamics become linearly unstable, we consider a small random perturbation to the fixed-point abundances $x_k^*(t) = x_k^* + \epsilon y_k(t)$. In the stable regime, this perturbation will decay to zero. In the unstable phase, the abundances will not in general return to x_k^* after being perturbed. In Appendix C, we find that such a perturbation will eventually decay to zero provided the following condition holds:

$$\frac{\sigma^2}{d^2} \sum_k p_k \frac{k^2 \chi_k^2}{\phi_k} < 1. \quad (7)$$

That is to say, the system is stable against linear perturbations if this inequality is satisfied, and is not otherwise.

Solving the fixed-point equations [Eqs. (4)] simultaneously with the condition obtained from setting the left-hand side of the inequality in Eq. (7) equal to one gives us the boundary of the stable and linearly unstable phase. In the fully connected

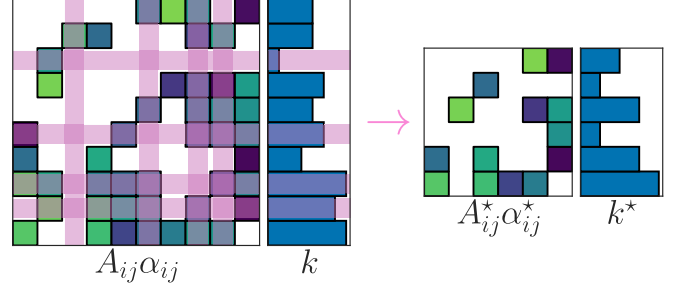


FIG. 3. Structure of the interaction matrix and corresponding degree sequence in the original pool of species vs their counterparts in the surviving community. Pink strips indicate which species go extinct in the course of the dynamics, and are hence removed from the community. In this example (counting from the top row of $A_{ij}\alpha_{ij}$), $S^* = \{1, 2, 4, 5, 7, 10\}$. The degree sequence among the survivors is not simply the sequence of original degrees restricted to surviving species, because some of the survivors' interaction partners also die out. Generally, the degree of any extant species in the surviving community will be lower than its original degree.

system, the condition for the onset of the linear instability reduces to $\sigma^2 \phi (1 + \gamma)^2 < 1$, which has been derived previously using both DMFT [32] and the static cavity method [33].

IV. PROPERTIES OF THE SURVIVING COMMUNITY

We have established the analytical theory for describing the overall properties of the surviving community, as well as the conditions under which this theory is valid. We now turn our attention to underlying statistics of the network and the interactions of surviving community. Specifically, in this section we will quantify how the survival rates, abundances, and interaction strengths between species depend on their connectivity.

Throughout this section, we write A^* , k_i^* , p^* , and α^* for the adjacency matrix, the degree (connectivity) of a species i , the degree distribution, and the matrix of interaction strengths in the surviving community, respectively. We also write N^* for the number of species in the surviving community, and S^* for the set of all persisting species. We emphasize that A^* , k_i^* , p^* , α^* are not the same as the corresponding quantities in the original community, A , k_i , p , α . The differences between the two are the result of the interaction-dependent species extinctions that occur during the course of the dynamics. The relationship between $A_{ij}\alpha_{ij}$, k_i and $A_{ij}^*\alpha_{ij}^*$, k_i^* is illustrated in Fig. 3.

A. Structure of the network

In this section we will use the statistics of A_{ij}^* to find expressions for the degree of a species in the *surviving* community, given its degree in the *original* community, as well as the degree distribution in the surviving community. One crucial observation that will aid us in doing this is the following. The probability of any two species interacting in the surviving community (i.e., conditioned on the survival of both species) is $kk'/(dN)$, where k, k' are the species degrees in the *original* community. This is because, to leading order in $1/d$,

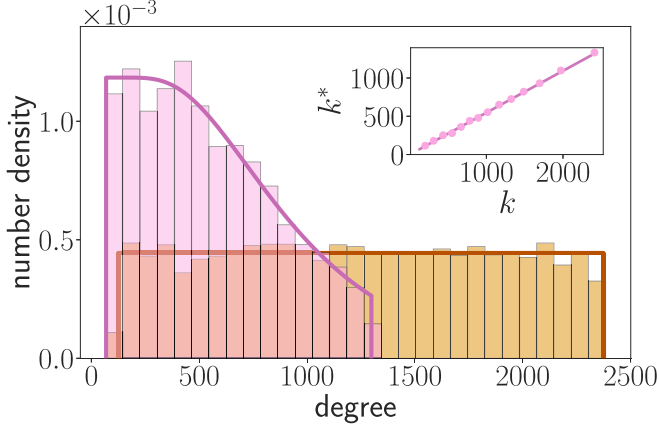


FIG. 4. Degree distribution in the surviving community (tall pink distribution) and the original species pool (flat orange distribution). The degree distribution in the original community is uniform, while the degree distribution in the surviving community is given by Eq. (9). Parameters are the same as Fig. 2(c). The inset shows the degree sequence in the surviving community as a function of the degree sequence in the original community. Bars and markers are computed from a single run of the dynamics with $N = 5000$. To avoid too many points in the inset, we only display markers for 1 in every 250 species in the surviving community. No average is taken.

the survival of different species can be treated as independent events. We discuss this in more detail in Appendix E.

One notes that although the conditional probability that species interact *given* their survival is trivially related to their interaction probability in the original pool (they are equal), the probability that both species actually survive is dependent on their respective degrees. This leads to nontrivial changes in the network structure.

The expected degree of a surviving species, given its degree in the original community, can be computed from our expression for the probability of any two species interacting in the surviving community (see Appendix E 3 for details). We find, for the expected degree,

$$E[k_i^* | k_i, i \in S^*] = rk_i, \quad (8)$$

where $E[\dots]$ denotes the combined average over \mathbf{A} and α , and where $r = \sum_k p_k \phi_k k / \sum_k p_k k$ is the survival probability of the neighbors of an arbitrarily chosen species in the original community. In Appendix E, we further show that the variance $E[(k_i^*)^2 | k_i, i \in S^*] - E[k_i^* | k_i, i \in S^*]^2$ is subleading in $1/d$. Hence, the probability distribution of species' degrees in the surviving community, given that they had degree k in the original community, is highly concentrated around the mean value given in Eq. (8). This can be seen in the Fig. 4 inset, which shows a scatter plot of the points (k_i^*, k_i) for $i \in S^*$ for one particular instance of \mathbf{A} and α (i.e., there is no average performed). We see an almost perfect linear relationship between k^* and k with very little fluctuation. From Eq. (8), the gradient of this line is r .

Using Eq. (8), we can find a compact expression for the degree distribution in the surviving community, $p_{k^*}^*$. We also use the fact that, for many possible degrees and large N , the integer spacing between different possible degrees effectively becomes a continuum. For this reason, we define

$P^*(k^*/N) = N p_{k^*}^*$ and $P(k/N) = N p_k$. We can express $P^*(\kappa^*)$ (where $\kappa^* = k^*/N$ is a variable between 0 and 1) in terms of the original degree distribution $P(\kappa)$ and survival rate as

$$P^*(\kappa^*) = \frac{1}{\phi r} \Phi\left(\frac{\kappa^*}{r}\right) P\left(\frac{\kappa^*}{r}\right), \quad (9)$$

where $\Phi(k/N) = \phi_k$. This can be understood as follows: the probability $P^*(\kappa^*)$ that a randomly selected species in the surviving community has degree k^* is proportional to the product of the probabilities that a randomly selected species in the initial pool has degree $k = k^*/r$ and that this species survives $[P(\kappa^*)\Phi(\kappa^*)]$. The factor of $1/(\phi r)$ is a normalization constant, ensuring that $\int P^*(\kappa^*) d\kappa^* = 1$ (see Appendix E 3 for details).

In Fig. 4, we show the effect of extinctions (brought about due to the constraint of feasibility) on a community interacting on a network that initially has a uniform degree distribution. It is clear that, relative to the initial degree distribution, there are more species with low degree than with high degree in the surviving community. This is driven by the fact that highly connected species in the original community are less likely to survive than species with low degree in competitive communities (i.e., for $\mu < 0$; see Appendix B and the next section for details).

Additionally, in Appendix F we show how Barabási-Albert networks are deformed by the extinction process. This also serves as a test of the validity of our approach to more general networks with weak degree correlations [53], to which an annealed network approximation is expected to apply [31,43]. Furthermore, we demonstrate in Appendix G how we can choose the initial degree distribution such that the final network of surviving species has a designated form. In particular, we produce a community whose final network of interactions is scale-free.

B. Survival rates and abundances as functions of degree

As we see in Fig. 5(a), species with higher initial degree are less likely to survive. This can be understood in broad terms from Eq. (3). The abundance x_k^* is a random variable drawn from a clipped Gaussian distribution. That is, if the Gaussian variable z is such that the right-hand side (RHS) of Eq. (3) is negative, the species does not survive. Given that the factor multiplying z is proportional to \sqrt{k} and that the factor multiplying $\mu < 0$ is proportional to k , we see that as k increases, it is more likely that the RHS of Eq. (3) is negative. Hence, a higher fraction of species go extinct for higher k . This is always the case for $\mu < 0$ (see Appendix B).

Figure 5(b) shows the expected abundance M_{k^*} of species as a function of their degree in the surviving community, which in the case shown is also seen to be a decreasing function of k^* . This is not always guaranteed to be the case, however, even for $\mu < 0$. With that being said, in Appendix B, we show that the region in parameter space for which the system is stable, where $\mu < 0$, and for which M_{k^*} and k^* are positively correlated, is small. Hence, for $\mu < 0$, only a small range of parameters could give rise to a community in which M_{k^*} is an increasing function of k^* . This general trend can once again be understood from Eq. (3), where we see that the

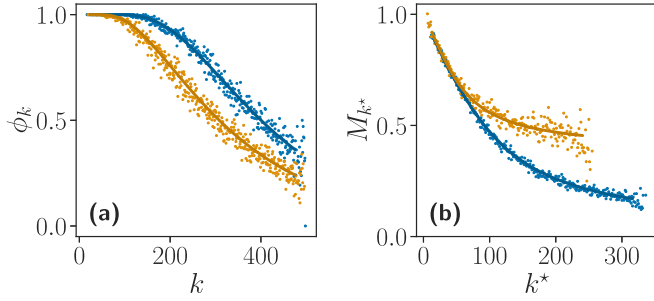


FIG. 5. (a) Survival rate as a function of degree in the original community. (b) Abundance as a function of degree in the surviving community. The survival rate is written as a function of degree in the original community, rather than as a function of degree in the surviving community. In contrast, the abundance of a species with a given degree is an observable that requires only information about the surviving community; hence we plot it as a function of k^* rather than k . The parameters are $\mu = -3$, $\sigma = 1.2$, $d = N/4$, $w = 0.45N$, $N = 2000$, and the values of γ and the corresponding colors are the same as in Fig. 2 (blue, $\gamma = -1$; orange, $\gamma = 0$). There is no curve with $\gamma = 1$, as the system is then unstable for the given parameters. In (b), the curves terminate at different values of k^* because of the differences in the limit of the degree sequence k^* in the surviving community. Markers are the average over 200 runs of the dynamics, and the solid lines are analytical predictions.

term proportional to μ , which determines the typical value of x_k^* , is also proportional to k .

The fact that ϕ_k and M_{k^*} are decreasing functions of degree has consequences for the relationship between species and their neighbors in the community. In Sec. IV A, we introduced the probability of survival of the neighbors of a species in the original community $r = \sum_k p_k \phi_k k / \sum_k p_k k$. We now show that if ϕ_k decreases with k , then $r < \phi$. That is, the probability of survival of the neighbors of a species is lower than the overall probability of species survival.

To see this, we first observe that if ϕ_k decreases with k , then the covariance of ϕ_k and k (computed with respect to the degree distribution p_k) must be negative. That is, $\sum_k p_k \phi_k k - (\sum_k p_k k)(\sum_{k'} p_{k'} \phi_{k'}) < 0$. We arrive at our claim after dividing both sides of the inequality by $\sum_k p_k k$ and recalling that $\phi = \sum_k p_k \phi_k$.

By an identical argument, we can conclude that if M_{k^*} is a decreasing function of k^* , then the average abundance of the neighbors of a species in the community is lower than the average abundance in the surviving community as a whole. Following the colloquial statement of the famous friendship paradox, "your friends are more popular than you are," we could say that "species' neighbors are less populous than they are."

In Appendix F, we show that these same trends of ϕ_k and M_{k^*} hold in the case of a Barabási-Albert network.

C. Interaction strengths in the surviving community

It is known that intricate correlations between interaction coefficients, which are not present in the original community, emerge in the surviving communities of fully connected GLV systems [33,36,37]. In this section, we show that in network GLV systems, the dynamics also induce correlations between the degree of a species and its interaction coefficients in the

surviving community, even though there are no such correlations in the initial community.

To quantify this effect, we characterize the strength of interactions "coming into" and "going out of" a species with degree k in a general network as

$$\begin{aligned}\mu_k^{\text{in}} &= \frac{d}{N_k} \sum_{i \in S_k} \frac{1}{k} \sum_j A_{ij} \alpha_{ij}, \\ \mu_k^{\text{out}} &= \frac{d}{N_k} \sum_{i \in S_k} \frac{1}{k} \sum_j A_{ji} \alpha_{ji},\end{aligned}\quad (10)$$

where we write S_k for the set of species that have degree k and N_k for the number of species in this set. Because the network and interaction strengths are independent in the original community, the ensemble average in and out interaction strengths are both equal to $\langle \mu_k^{\text{in/out}} \rangle_{A,\alpha} = \mu$ for any value of k . However, as Fig. 6 demonstrates, when we measure these same quantities in the surviving community [i.e., $\mu_k^{\text{in}} = (d^*/N_k^*) \sum_{i \in S_k^*} \sum_{j \in S_k^*} A_{ij}^* \alpha_{ij}^* / k^*$ and similar for μ_k^{out}], we find that they depend on the degree k^* .

We can understand the relationship between the in and out interaction strengths and connectivity by examining Fig. 6(b). In this case, $\gamma = 0$, and therefore there is no imposed correlation between the in (α_{ij}) and out (α_{ji}) interaction coefficients, so we are better able to disentangle the effects at play. We remind the reader that we consider competitive interactions with $\mu < 0$.

Let us begin with the incoming interactions. We see that the average incoming interaction becomes less negative with degree k^* . We attribute this primarily to the differing survival rate of species, depending on degree. We can see this as follows. Almost all species with small k survive (i.e., $\phi_k \approx 1$), and so we expect the average incoming interactions to be same in the surviving and initial communities for species with small k^* (i.e., $\mu_{k^*}^{\text{in}} \approx \mu$). With increasing value of k^* , the survival rate of the species decreases (see Fig. 5). Because the species that survive are those with the most favorable interactions, we find the upwards trend of $\mu_{k^*}^{\text{in}}$ with k^* .

The average outgoing interaction strength exhibits the opposite trend to the incoming interaction strength in Fig. 6(b). That is, low-degree species have more positive outgoing interactions than high-degree species. This can be explained as follows. First we note that low-degree species have higher abundance (see Sec. IV B), and therefore have a greater impact on the probability of their neighbors' survival. This means that the neighbors of low-degree species are more likely to go extinct than neighbors of species with high degree (which have comparatively low abundance). As was the case with the incoming interactions, it is those species who interact more favorably that survive. Because neighbors of species with low degree are more likely to go extinct, $\mu_{k^*}^{\text{out}}$ is a decreasing function of k^* .

The trends in the other panels of Fig. 6 can be understood as a kind of superposition of the trends in Fig. 6(b), since a nonzero γ connotes a correlation between the incoming and outgoing interactions of a species. For example, when $\gamma = 1$, the outgoing and incoming interactions must be identical. Hence, $\mu_{k^*}^{\text{out}} = \mu_{k^*}^{\text{in}}$ and the corresponding curve in Fig. 6(c) is seen to be an "average" of the upwards and the downwards

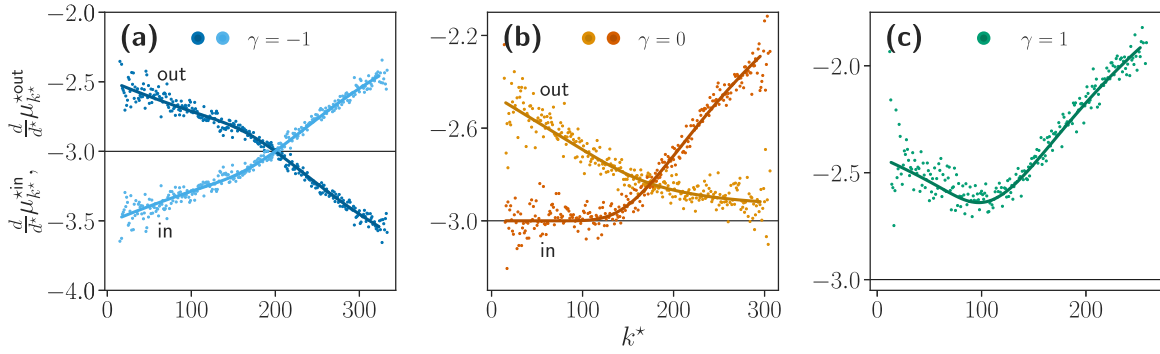


FIG. 6. Average "in" and "out" interaction strength as a function of degree in the surviving community with (a), (b), and (c) corresponding to $\gamma = (-1, 0, 1)$, respectively. In (a) and (b), the curves with positive gradient show the "in" interaction strengths and the curves with negative gradient show the "out" interaction strengths. In (c), the in and out interactions are exactly equal. A horizontal black line has been added to all panels to indicate the mean interaction strength in the original community. Parameters are $\mu = -3$, $\sigma = 0.6$, $d = N/4$, $w = 0.45N$, $N = 2000$. Markers are the average of 200 runs of the simulation. Solid lines are analytical predictions (see Appendix D for the explicit expressions).

trends in Fig. 6(b). On the other hand, for $\gamma = -1$, the fluctuations in the incoming and outgoing interactions are exactly the negative of each other [i.e., $\alpha_{ij} - \mu/d = -(\alpha_{ji} - \mu/d)$], hence the mirror-image effect in Fig. 6(a).

Although we have provided a qualitative rationale of the trends in Fig. 6, we are also able to provide direct quantitative evidence of their causation using the cavity method (in a similar way to Refs. [36,37]). That is, we see directly how the survival bias of species affects the incoming interactions, and how the species abundance affects the outgoing interactions. The cavity method also yields the analytical results in Fig. 6. The details are technical, and so we direct the interested reader to Appendix D for more information.

V. DISCUSSION

In this work, we have studied an extension of the popular generalized Lotka-Volterra equations by incorporating random network structure with an arbitrary degree distribution. We have found that the network and interaction statistics of the surviving community differ greatly from those of the original community. This demonstrates that the condition of feasibility, which linear models cannot guarantee, is a strong constraint on the structure of ecological networks. To derive our central results, we extended the usual dynamical mean-field theory for generalized Lotka-Volterra dynamics to describe heterogeneous interaction statistics, in a similar way to our previous work in Ref. [44].

Most importantly, we demonstrated that, in the surviving community, there are correlations between the connectivity of a species and its interaction coefficients. These correlations are a fingerprint of the dynamics, which results from constraining a subset of the original species to coexist, and they are not present in the initial pool of species from which the surviving community is formed.

Direct tests of the relations between the network and resulting interaction statistics in real ecological communities could in principle be attempted using modern inference techniques [54–56]. While the network structure of natural ecosystems might differ from the assumptions in our model, and inferring interaction coefficients for high-dimensional models such as

ours is not straightforward, it might still be possible to verify some of our predictions, at least qualitatively. Perhaps the most easily tested prediction in the current work, since it does not involve measuring precise interaction coefficients, is the one similar to the friendship paradox, namely, that the neighbors of species in the interaction network typically have a lower abundance than the focal species.

By finding an expression for the degree distribution in the surviving community, we were able to go beyond community-wide properties to probe how degree-dependent statistics vary across the community. We found that, for a wide range of model parameters, the survival rates and abundance of species are negatively correlated with their degree. This in turn implied that a given species' neighbors were more likely to survive, and were more abundant on average, than said species. We also found that the degree distribution in the surviving community contained relatively few species with high degree, and more species with low degree, than in the original community. This offers a possible explanation for this same trend found in real ecological networks [23,57,58], namely, that a skewed degree distribution may partially be a consequence of a community's feasibility.

We note that in Ref. [59], Serván *et al.* observe that network structure plays only a small role in the outcome of the final community composition (specifically, the average survival rate) in a related version of the Lotka-Volterra model. In the aforementioned work, species have varying intrinsic growth rates, which can be negative and turn into an effective death rate. Hence, species can be driven to extinction even in the absence of interactions. In Ref. [59] it is thus mostly the intrinsic growth (or death) rate of a species that determines survival, and the network structure plays a secondary role. In our work, intrinsic growth rates are all positive and do not vary across species. If there are no interactions, all species survive. The survival of a species is thus determined solely by its interactions. Hence, the network has a more pronounced effect. Loosely speaking, Ref. [59] and our work can be seen as analyzing two extremes on a scale of comparatively less influential interactions to strongly influential interactions. As one increases the significance of interactions in the model, one sees that the precise network

structure has more of an effect on the nature of the surviving community.

There are many opportunities for extensions to this work. Our model incorporates only the most simple random network model, but real ecological networks are known to be much more complex. It would be interesting to see how additional structures, such as assortativity, intervality, or particular motifs in the initial network of interactions, are modified when we constrain the network to be that of a feasible equilibrium [60–64]. We also know that ecological networks consist of both directed and undirected links (that is, the adjacency matrix is not symmetric in general) [65,66], which would pose a simple mathematical extension to the present work. Finally, ecological networks are known to straddle the line between being dense and sparse, with connectivity widely reported to be in the range 0.05–0.3 [11,23]. Our work could be extended to include sparse corrections for the case where the connectivity is very low (using techniques similar to, e.g., Ref. [67]). In particular, we expect a sparse surviving network to have more significant degree correlations than the dense model, which would perhaps offer a mechanism for the disassortativity found in real ecological networks [65].

Note added. We would like to highlight Refs. [38,39], which address a similar topic to our own work. While all three papers employ a "heterogeneous mean-field approximation," the focus of each work is quite different. In particular, Refs. [38,39] do not study the structure of the surviving community network. Instead, they characterize in detail the rates of survival of species in the initial community, as we will now briefly describe.

Reference [39] demonstrates a nonmonotonic relationship between survival rate and mean interaction strength. In particular, it is possible for the survival rate to decrease for more cooperative communities, rather counter to intuition, and also

that survival probability can have a minimum as a function of connectivity.

The author of Ref. [38] makes the observation that purely competitive or purely cooperative communities (in which $\sigma = 0$) require species to have a maximum or minimum (respectively) connectivity in order to survive. It is also shown how this can be used to explain survival rates in heterogeneously interacting communities ($\sigma > 0$). The author also studies the phase with diverging abundances, and connections with economics are made via the calculation of Gini coefficients.

ACKNOWLEDGMENTS

We acknowledge support from the Agencia Estatal de Investigación and Fondo Europeo de Desarrollo Regional (FEDER, UE) under Project APASOS (PID2021-122256NB-C21, PID2021-122256NB-C22). This work was partially supported by the María de Maeztu Project CEX2021-001164-M funded by the MICIU/AEI/10.13039/501100011033. We further acknowledge the award of a studentship by the Engineering and Physical Sciences Research Council EPSRC. J.W.B. is supported by grants from the Simons Foundation (Grant No. 454935 Giulio Biroli). J.W.B. also thanks the Leverhulme Trust for support through the Leverhulme Early Career Fellowship scheme.

APPENDIX A: DERIVATION OF THE DMFT EFFECTIVE DYNAMICAL EQUATIONS

To derive an effective set of mean-field equations describing the time dependence of species abundances in the community, we start with the Martin-Siggia-Rose-Janssen-de Dominicis (MSRJD) [49–51,68] generating functional of the Generalized Lotka-Volterra (GLVE) dynamics in Eq. (1)

$$Z[\psi] = \int \mathcal{D}\mathbf{x} \mathcal{D}\widehat{\mathbf{x}} \exp \left[i \sum_i \int dt \widehat{x}_i(t) \left(\frac{\dot{x}_i(t)}{x_i(t)} - 1 + x_i(t) - \sum_j A_{ij} \alpha_{ij} x_j(t) - h_i(t) \right) + i \sum_i \int dt x_i(t) \psi_i(t) \right], \quad (\text{A1})$$

where the adjacency matrix \mathbf{A} and interaction matrix $\boldsymbol{\alpha}$ are described in the main text. The functions $h_i(t)$ and $\psi_i(t)$ do not appear in the dynamics in Eq. (1). These are source fields that are set to zero at the end of the calculation. We will average $Z[\psi]$ over the distribution of both the network (\mathbf{A}) and the interactions ($\boldsymbol{\alpha}$). Like in Ref. [32], the resulting disorder-averaged functional can then be manipulated into a form that is recognizable as the generating functional of a different, decoupled set of dynamical equations. This set of equations describes the time dependence of the abundance of a typical species with degree k in the original community.

All the disorder in Eq. (A1) is in the term containing the interaction coefficients $A_{ij}\alpha_{ij}$. The average of this term over the distributions of $\boldsymbol{\alpha}$ and \mathbf{A} is carried out as follows:

$$\begin{aligned} \left\langle \exp \left[i \sum_{ij} \int dt A_{ij} \alpha_{ij} \widehat{x}_i(t) x_j(t) \right] \right\rangle_{\mathbf{A}, \boldsymbol{\alpha}} &= \prod_{i < j} \left\langle \exp \left[i \int dt A_{ij} (\alpha_{ij} \widehat{x}_i(t) x_j(t) + \alpha_{ji} \widehat{x}_j(t) x_i(t)) \right] \right\rangle_{A_{ij}, (\alpha_{ij}, \alpha_{ji})} \\ &= \prod_{i < j} \left(1 + \frac{k_i k_j}{dN} \left(\left\langle \exp \left[i \int dt (\alpha \widehat{x}_i(t) x_j(t) + \beta \widehat{x}_j(t) x_i(t)) \right] \right\rangle_{(\alpha, \beta)} - 1 \right) \right) \\ &= \exp \left[\frac{1}{2} \sum_{ij} \ln \left(1 + \frac{k_i k_j}{dN} \left(\left\langle \exp \left[i \int dt (\alpha \widehat{x}_i(t) x_j(t) + \beta \widehat{x}_j(t) x_i(t)) \right] \right\rangle_{(\alpha, \beta)} - 1 \right) \right) \right], \end{aligned} \quad (\text{A2})$$

where we have written $\langle \cdots \rangle_{\mathbf{A}, \alpha}$ for a joint average over all elements of the matrices \mathbf{A} and α , and $\langle \cdots \rangle_{(\alpha_{ij}, \alpha_{ji})}$ for the average over the joint distribution of the specific elements α_{ij} and α_{ji} . The joint distribution of $(\alpha_{ij}, \alpha_{ji})$ does not depend on i or j , as the pairs $(\alpha_{ij}, \alpha_{ji})$ are drawn independently for each i and j . To make this lack of dependence explicit, we have replaced $\alpha_{ij} \rightarrow \alpha$ and $\alpha_{ji} \rightarrow \beta$ between the second and the third lines.

To decouple the i and j indices from the final expression in Eq. (A2), for each degree k in the original community network, we introduce the following functional:

$$P_k[\mathbf{x}, \hat{\mathbf{x}}] = \frac{1}{N_k} \sum_{i \in S_k} \prod_t \delta(x(t) - x_i(t)) \delta(\hat{x}(t) - \hat{x}_i(t)), \quad (\text{A3})$$

where $i \in S_k$ indicates that species i has degree k in the original community and $N_k = p_k N$ is the number of species with degree k in the original community [p_k is the degree distribution in the original community]. For each k , the functional $P_k[\mathbf{x}, \hat{\mathbf{x}}]$ is the probability that the functions $x(t)$ and $\hat{x}(t)$ are equal to the functions $x_i(t)$ and $\hat{x}_i(t)$, respectively, which are constrained to follow the dynamics of species with degree k . With this definition, we can write the disordered part of the generating functional as

$$\begin{aligned} \left\langle \exp \left[i \sum_{ij} \int dt A_{ij} \alpha_{ij} \hat{x}_i(t) x_j(t) \right] \right\rangle_{\mathbf{A}, \alpha} &= \exp \left[\frac{N^2}{2} \sum_{kk'} p_k p_{k'} \int \mathcal{D}\mathbf{x} \mathcal{D}\hat{\mathbf{x}} \mathcal{D}\mathbf{y} \mathcal{D}\hat{\mathbf{y}} P_k[\mathbf{x}, \hat{\mathbf{x}}] \mathbf{P}_{k'}[\mathbf{y}, \hat{\mathbf{y}}] \right. \\ &\quad \times \ln \left(1 + \frac{kk'}{dN} \left(\left\langle \exp \left[i \int dt (\alpha \hat{x}(t) y(t) + \beta \hat{y}(t) x(t)) \right] \right\rangle_{(\alpha, \beta)} - 1 \right) \right) \Bigg]. \quad (\text{A4}) \end{aligned}$$

We enforce the definition of $P_k[\mathbf{x}, \hat{\mathbf{x}}]$ by inserting delta functions in their complex exponential form into the generating functional:

$$\begin{aligned} 1 &\propto \int \mathcal{D}P_k \mathcal{D}\hat{P}_k \exp \left[i \sum_k N_k \int \mathcal{D}\mathbf{x} \mathcal{D}\hat{\mathbf{x}} \hat{P}_k[\mathbf{x}, \hat{\mathbf{x}}] \left(P_k[\mathbf{x}, \hat{\mathbf{x}}] - \frac{1}{N_k} \sum_{i \in S_k} \prod_t \delta(x(t) - x_i(t)) \delta(\hat{x}(t) - \hat{x}_i(t)) \right) \right], \\ &\propto \int \mathcal{D}P_k \mathcal{D}\hat{P}_k \exp \left[i \sum_k N_k \int \mathcal{D}\mathbf{x} \mathcal{D}\hat{\mathbf{x}} \hat{P}_k[\mathbf{x}, \hat{\mathbf{x}}] P_k[\mathbf{x}, \hat{\mathbf{x}}] - i \sum_{i \in S_k} \hat{P}_k[x_i, \hat{x}_i] \right]. \quad (\text{A5}) \end{aligned}$$

With these definitions enforced, the disorder-averaged generating functional of Eq. (1) takes the following form:

$$\begin{aligned} \langle Z[\Psi] \rangle_{\mathbf{A}, \alpha} &\propto \int \mathcal{D}\mathbf{x} \mathcal{D}\hat{\mathbf{x}} \mathcal{D}P \mathcal{D}\hat{P} \exp \left[i \sum_i \int dt \hat{x}_i(t) \left(\frac{\dot{x}_i(t)}{x_i(t)} - 1 + x_i(t) - h_i(t) \right) + i \sum_i \int dt x_i(t) \psi_i(t) \right] \\ &\quad \times \exp \left[\frac{N^2}{2} \sum_{kk'} p_k p_{k'} \int \mathcal{D}\mathbf{x} \mathcal{D}\hat{\mathbf{x}} \mathcal{D}\mathbf{y} \mathcal{D}\hat{\mathbf{y}} P_k[\mathbf{x}, \hat{\mathbf{x}}] \mathbf{P}_{k'}[\mathbf{y}, \hat{\mathbf{y}}] \right. \\ &\quad \times \ln \left(1 + \frac{kk'}{dN} \left(\left\langle \exp \left[i \int dt (\alpha \hat{x}(t) y(t) + \beta \hat{y}(t) x(t)) \right] \right\rangle_{(\alpha, \beta)} - 1 \right) \right) \Bigg] \\ &\quad \times \exp \left[iN \sum_k p_k \int \mathcal{D}\mathbf{x} \mathcal{D}\hat{\mathbf{x}} \hat{P}_k[\mathbf{x}, \hat{\mathbf{x}}] P_k[\mathbf{x}, \hat{\mathbf{x}}] - i \sum_{i \in S_k} \hat{P}_k[x_i, \hat{x}_i] \right]. \quad (\text{A6}) \end{aligned}$$

To proceed, we could explicitly perform the average over the joint distribution of the interaction strengths (α, β) and simplify the resulting expression. If we do this for the interaction statistics in Eq. (2), to leading order in powers of $1/d$, the integrand is of the form $\exp[NS]$. The integral can then be evaluated with a saddle-point approximation for large N . Even though our interest in the main text is in dense networks, where retaining only leading terms in powers of $1/d$ is valid, we can proceed without having to make this assumption. That is, we can evaluate the integral with a saddle-point equation without assuming the network is dense. To do this, we simply assume that the term with a prefactor of N^2 in the integrand is $O(N)$. With this assumption, the following functional (proportional to the joint cumulant generating function of $A_{ij}\alpha_{ij}$ and $A_{ji}\alpha_{ji}$) is $O(N^0)$ for each k and k' :

$$f_{kk'}[\mathbf{x}, \hat{\mathbf{x}}, \mathbf{y}, \hat{\mathbf{y}}] = N \ln \left(1 + \frac{kk'}{dN} \left(\left\langle \exp \left[i \int dt (\alpha \hat{x}(t) y(t) + \beta \hat{y}(t) x(t)) \right] \right\rangle_{(\alpha, \beta)} - 1 \right) \right) \stackrel{\text{assumption}}{=} O(N^0). \quad (\text{A7})$$

We note that if this functional is not $O(N^0)$, then the following steps in our derivation are not valid. This assumption is very similar to that in Ref. [69] in that we make an assumption about the large- N behavior of a cumulant generating function of the interaction coefficients, rather than of the coefficients themselves. Our expression for the disorder-averaged generating functional

now reads (the definition of $f_{kk'}$ is just notation, we do not enforce its definition with delta functions)

$$\begin{aligned} \langle Z[\boldsymbol{\psi}] \rangle_{\mathbf{A}, \alpha} &\propto \int \mathcal{D}P \mathcal{D}\hat{P} \\ &\times \exp \left[\frac{N}{2} \sum_{kk'} p_k p_{k'} \int \mathcal{D}\mathbf{x} \mathcal{D}\hat{\mathbf{x}} \mathcal{D}\mathbf{y} \mathcal{D}\hat{\mathbf{y}} P_k[\mathbf{x}, \hat{\mathbf{x}}] \mathbf{P}_{k'}[\mathbf{y}, \hat{\mathbf{y}}] \mathbf{f}_{kk'}[\mathbf{x}, \hat{\mathbf{x}}, \mathbf{y}, \hat{\mathbf{y}}] \right] \\ &\times \exp \left[iN \sum_k p_k \int \mathcal{D}\mathbf{x} \mathcal{D}\hat{\mathbf{x}} \hat{P}_k[\mathbf{x}, \hat{\mathbf{x}}] \mathbf{P}_k[\mathbf{x}, \hat{\mathbf{x}}] \right] \\ &\times \exp \left[N \sum_k p_k \ln \int \mathcal{D}\mathbf{x} \mathcal{D}\hat{\mathbf{x}} \exp \left[i \int dt \hat{x}(t) \left(\frac{\dot{x}(t)}{x(t)} - 1 + x(t) - h_k(t) \right) - i\hat{P}_k[\mathbf{x}, \hat{\mathbf{x}}] + i \int dt x(t) \psi_k(t) \right] \right], \quad (\text{A8}) \end{aligned}$$

where we have supposed that $h_i(t)$ and $\psi_i(t)$ only depend on the degree of species i in order to be able to factorize the final term. That is, $h_i(t) = h_k(t)$ and $\psi_i(t) = \psi_k(t)$ for all species i with degree k . We can evaluate this integral with a saddle-point approximation for large N . First, taking the derivative of the exponent with respect to the hatted functionals \hat{P}_k gives

$$P_k[\mathbf{x}, \hat{\mathbf{x}}] = \frac{\exp \left[i \int dt \hat{x}_k(t) \left(\frac{\dot{x}_k(t)}{x_k(t)} - 1 + x_k(t) - h_k(t) \right) - i\hat{P}_k[\mathbf{x}_k, \hat{\mathbf{x}}_k] + i \int dt x_k(t) \psi_k(t) \right]}{\int \mathcal{D}\mathbf{x} \mathcal{D}\hat{\mathbf{x}} \exp \left[i \int dt \hat{x}(t) \left(\frac{\dot{x}(t)}{x(t)} - 1 + x(t) - h_k(t) \right) - i\hat{P}_k[\mathbf{x}, \hat{\mathbf{x}}] + i \int dt x(t) \psi_k(t) \right]}, \quad (\text{A9})$$

where the subscript in $x_k(t)$ indicates that the abundance $x_k(t)$ is constrained to be the trajectory of a typical species with degree k ; we justify this interpretation further on in the derivation. The unhatted saddle equation (taking derivatives of the exponent with respect to P_k) is

$$\hat{P}_k[\mathbf{x}, \hat{\mathbf{x}}] = i \sum_{k'} p_{k'} \int \mathcal{D}\mathbf{y} \mathcal{D}\hat{\mathbf{y}} P_{k'}[\mathbf{y}, \hat{\mathbf{y}}] \mathbf{f}_{kk'}[\mathbf{x}, \hat{\mathbf{x}}, \mathbf{y}, \hat{\mathbf{y}}]. \quad (\text{A10})$$

Substituting Eq. (A9) into Eq. (A10), we arrive at the following self-consistent functional equation for \hat{P}_k :

$$\hat{P}_k[\mathbf{x}, \hat{\mathbf{x}}] = i \sum_{k'} p_{k'} \frac{\int \mathcal{D}\mathbf{y} \mathcal{D}\hat{\mathbf{y}} f_{kk'}[\mathbf{x}, \hat{\mathbf{x}}, \mathbf{y}, \hat{\mathbf{y}}] \exp \left[i \int dt \hat{y}(t) \left(\frac{\dot{y}(t)}{y(t)} - 1 + y(t) - h_{k'}(t) \right) - i\hat{P}_{k'}[\mathbf{y}, \hat{\mathbf{y}}] + i \int dt y(t) \psi_{k'}(t) \right]}{\int \mathcal{D}\mathbf{y} \mathcal{D}\hat{\mathbf{y}} \exp \left[i \int dt \hat{y}(t) \left(\frac{\dot{y}(t)}{y(t)} - 1 + y(t) - h_{k'}(t) \right) - i\hat{P}_{k'}[\mathbf{y}, \hat{\mathbf{y}}] + i \int dt y(t) \psi_{k'}(t) \right]}. \quad (\text{A11})$$

We now rewrite this as

$$\hat{P}_k[\mathbf{x}, \hat{\mathbf{x}}] = i \sum_{k'} p_{k'} \langle f_{kk'}[\mathbf{x}, \hat{\mathbf{x}}, \mathbf{y}, \hat{\mathbf{y}}] \rangle_{k'}^{(y)}, \quad (\text{A12})$$

where $\langle \cdots \rangle_k^{(y)}$ stands for the ratio of functional integrals in Eq. (A11), with (\cdots) in place of $f_{kk'}[\mathbf{x}, \hat{\mathbf{x}}, \mathbf{y}, \hat{\mathbf{y}}]$. In particular, we point out that this means the quantity $\langle f_{kk'}[\mathbf{x}, \hat{\mathbf{x}}, \mathbf{y}, \hat{\mathbf{y}}] \rangle_y$ does not depend on arguments $\mathbf{y}, \hat{\mathbf{y}}$, or y , but it *does* depend on the degree k . To interpret $\langle \cdots \rangle_k^{(y)}$, we compare functional derivatives of the expression for Z in Eqs. (A1) and (A8) with respect to $\psi_i(t)$ and $h_i(t)$ to find (in the limit of large N)

$$\langle x(t) \rangle_k = -i \frac{1}{N_k} \sum_{i \in S_k} \frac{\partial \langle Z[\boldsymbol{\psi}] \rangle_{\mathbf{A}, \alpha}}{\partial \psi_i(t)} \Big|_{h=\psi=0} = \frac{1}{N_k} \sum_{i \in S_k} \langle x_i(t) \rangle_{\mathbf{A}, \alpha}, \quad (\text{A13})$$

$$\langle \hat{x}(t) \rangle_k = i \frac{1}{N_k} \sum_{i \in S_k} \frac{\partial \langle Z[\boldsymbol{\psi}] \rangle_{\mathbf{A}, \alpha}}{\partial h_i(t)} \Big|_{h=\psi=0} = \frac{1}{N_k} \sum_{i \in S_k} \langle \hat{x}_i(t) \rangle_{\mathbf{A}, \alpha}, \quad (\text{A14})$$

$$\langle \hat{x}(t) x(t') \rangle_k = -\frac{1}{N_k} \sum_{i \in S_k} \frac{\partial \langle Z[\boldsymbol{\psi}] \rangle_{\mathbf{A}, \alpha}}{\partial h_i(t)} \psi_i(t') \Big|_{h=\psi=0} = \frac{1}{N_k} \sum_{i \in S_k} \langle \hat{x}_i(t) x_i(t') \rangle_{\mathbf{A}, \alpha}, \quad (\text{A15})$$

where we have dropped the superscripts (x) in, e.g., $\langle x(t) \rangle_k^{(x)}$ on the left-hand side (LHS) of the above equations as there is only one dynamical variable which could be averaged over. We can do the same calculation for any other powers of $x(t)$ and $\hat{x}(t)$. Hence, $\langle x(t) \rangle_k$ is, in the large- N limit, equal to the average abundance of species with degree k in the community. Furthermore, because $Z[\boldsymbol{\psi} = 0] = 1$ [Eq. (A1)] is the integral of a delta function when $\psi_i(t) = 0$, derivatives of Z with respect to factors of \mathbf{h} only are all zero. Therefore, any averages containing only hatted variables vanish.

At the saddle point, we can finally write the disorder-averaged generating functional as

$$\begin{aligned} \langle Z[\Psi] \rangle_{\mathbf{A}, \alpha} &\propto \int \mathcal{D}\mathbf{x} \mathcal{D}\widehat{\mathbf{x}} \exp \left[i \sum_k p_k \int dt \widehat{x}_k(t) \left(\frac{\dot{x}_k(t)}{x_k(t)} - 1 + x_k(t) - h_k(t) \right) \right] \\ &\times \exp \left[\sum_{kk'} p_k p_{k'} \langle f_{kk'}[\mathbf{x}_k, \widehat{\mathbf{x}}_k, \mathbf{y}, \widehat{\mathbf{y}}] \rangle_{k'}^{(y)} + i \sum_k p_k \int dt x_k(t) \psi_k(t) \right]. \end{aligned} \quad (\text{A16})$$

We now evaluate the functional $f_{kk'}[\mathbf{x}, \widehat{\mathbf{x}}, \mathbf{y}, \widehat{\mathbf{y}}]$, with the random matrix α as described in Sec. II of the main text. To leading order in $1/N$ and $1/d$, we find

$$\begin{aligned} f_{kk'}[\mathbf{x}_k, \widehat{\mathbf{x}}_k, \mathbf{y}, \widehat{\mathbf{y}}] &= i \frac{kk' \mu}{d^2} \int dt (\widehat{x}_k(t) y(t) + \widehat{y}(t) x_k(t)) \\ &- \frac{kk' \sigma^2}{2d^2} \left[\left(\int dt \widehat{x}_k(t) y(t) \right)^2 + \left(\int dt \widehat{y}(t) x_k(t) \right)^2 \right] - \frac{kk' \gamma \sigma^2}{d^2} \int dt dt' \widehat{x}_k(t) y(t) \widehat{y}(t') x_k(t'). \end{aligned} \quad (\text{A17})$$

Averaging over the dynamics of y , and recalling that averages over only hatted variables equate to zero, we are left with

$$\langle f_{kk'}[\mathbf{x}_k, \widehat{\mathbf{x}}_k, \mathbf{y}, \widehat{\mathbf{y}}] \rangle_{k'}^{(y)} = i \frac{kk' \mu}{d^2} \int dt \widehat{x}_k(t) \langle y(t) \rangle_{k'} - \frac{kk' \sigma^2}{2d^2} \int dt dt' (\widehat{x}_k(t) \widehat{x}_k(t') \langle y(t) y(t') \rangle_{k'} + 2 \gamma \widehat{x}_k(t) x_k(t') \langle y(t) \widehat{y}(t') \rangle_{k'}). \quad (\text{A18})$$

Substituting this into Eq. (A16), we recognize $\langle Z[\Psi] \rangle_{\mathbf{A}, \alpha}$ as the generating functional of the following set of effective dynamical equations:

$$\dot{x}_k(t) = x_k(t) \left(1 - x_k(t) + \frac{\mu k}{d^2} \sum_{k'} p_{k'} k' M_{k'}(t) + \frac{\gamma \sigma^2 k}{d^2} \sum_{k'} p_{k'} k' \int dt G_{k'}(t, t') x_k(t') + \eta_k(t) \right), \quad (\text{A19})$$

where we have set $h_k(t) = 0$ and written $\langle y(t) \rangle_k = M_k(t)$ and $-i \langle \widehat{y}(t') y(t) \rangle_k = G_k(t, t')$. The quantities $M_k(t)$, $G_k(t, t')$, and the colored Gaussian noise term $\eta_k(t)$ are determined self-consistently via the following equations:

$$\langle \eta_k(t) \rangle_\eta = 0, \quad \langle \eta_k(t) \eta_l(t') \rangle_\eta = \delta_{kl} \frac{\sigma^2 k}{d^2} \sum_{k'} p_{k'} k' \langle x_k(t) x_{k'}(t') \rangle_\eta, \quad M_k(t) = \langle x_k(t) \rangle_\eta, \quad G_k(t, t') = \frac{\delta \langle x_k(t) \rangle_\eta}{\delta \eta_k(t')}. \quad (\text{A20})$$

The last of these relationships follows from writing down the generating functional of the effective dynamics Eq. (A19) without performing the average over the noise term $\eta_k(t)$ [which would simply return Eq. (A16)]. From this functional, it is then clear that differentiation with respect to the noise term "pulls down" a factor of $-\widehat{x}_k(t)$; hence we can replace factors of $-\widehat{x}_k(t)$ in Eq. (A16) with derivatives with respect to the noise.

1. Fixed-point equations

As discussed in the main text, we can derive a closed set of self-consistent equations for the abundance distribution in

the surviving community at a fixed point of the dynamics. Suppose that the dynamics in Eq. (A19) reaches a fixed point x_k^* . In this case, the noise term will be a static, mean zero Gaussian random variable with variance $\sigma^2 k / d^2 \sum_{k'} p_{k'} k' q_k$, with $q_k = \langle (x_k^*)^2 \rangle_z$. We also assume that the system's response function is a function of time differences only in this regime, so that $G_k(t, t') = G_k(t - t')$, which means we can write $\int dt' G_k(t, t') x_k(t') = \chi_k x_k^*$ for $\chi_k = \int d\tau g_k(\tau)$. The fixed-point abundance distribution of x_k^* is then given by (we have added back in the factor of h from the original generating functional so that we can cleanly write down the definition of χ_k)

$$x_k^*(z) = \max \left(0, \frac{1 + \mu k \sum_{k'} p_{k'} k' M_{k'} / d^2 + z \sigma \sqrt{k \sum_{k'} p_{k'} k' q_{k'}} / d + h}{1 - \gamma \sigma^2 k \sum_{k'} p_{k'} k' \chi_{k'} / d^2} \right). \quad (\text{A21})$$

By carefully evaluating the definitions of the parameters M_k , q_k , and χ_k , we arrive at the fixed-point equations in the main text, which we repeat here:

$$M_k = \int_{x_k^* > 0} dz f(z) x_k^*(z), \quad q_k = \int_{x_k^* > 0} dz f(z) x_k^*(z)^2, \quad \chi_k = \int_{x_k^* > 0} dz f(z) \frac{\partial x_k^*(z)}{\partial h}, \quad (\text{A22})$$

where $f(z) = \exp(-z^2/2) / \sqrt{2\pi}$ is the probability density function of the standard normal distribution.

We now expand out the definitions in Eqs. (A22) to find the explicit set of equations which we can numerically solve.

Expanding the definitions gives [note that the integration region $x_k^* > 0$ needs to be converted into an integration region over z using Eq. (A21)]

$$\begin{aligned}\chi_k &= \frac{w_0(\Delta_k)}{1 - \frac{\gamma\sigma^2 k}{d^2} \sum_{k'} p_{k'} k' \chi_{k'}}, \\ M_k &= \Sigma_k w_1(\Delta_k), \\ q_k &= \Sigma_k^2 w_2(\Delta_k),\end{aligned}\quad (\text{A23})$$

where we have defined the shorthands

$$\begin{aligned}\Sigma_k &= \frac{\sigma \sqrt{k} \sum_{k'} p_{k'} k' q_{k'} / d}{1 - \gamma \sigma^2 k \sum_{k'} p_{k'} k' \chi_{k'} / d^2}, \\ \Delta_k &= \frac{1 + \mu k \sum_{k'} p_{k'} k' M_{k'} / d^2}{\sigma \sqrt{k} \sum_{k'} p_{k'} k' q_{k'} / d}, \\ w_l(\Delta_k) &= \int_{-\infty}^{\Delta_k} dz f(z) (\Delta_k - z)^l.\end{aligned}\quad (\text{A24})$$

We also define the probability of survival for species that have degree k in the original community,

$$\phi_k = \int_{x_k^* > 0} dz f(z), \quad (\text{A25})$$

as well as the community-wide abundance and survival probability,

$$M = \sum_k p_k M_k, \quad \phi = \sum_k p_k \phi_k. \quad (\text{A26})$$

Equations (A23) can be numerically solved to find the fixed-point parameters for specific degree k . The integrals defining $w_l(\Delta_k)$ can be explicitly evaluated. For $l = 0, 1, 2$ we have

$$\begin{aligned}w_0(x) &= \frac{1}{2} \left(1 + \operatorname{erf} \left(\frac{x}{\sqrt{2}} \right) \right), \\ w_1(x) &= P(x) + \frac{1}{2} x \left(1 + \operatorname{erf} \left(\frac{x}{\sqrt{2}} \right) \right), \\ w_2(x) &= x P(x) + \frac{1}{2} (1 + x^2) \left(1 + \operatorname{erf} \left(\frac{x}{\sqrt{2}} \right) \right).\end{aligned}\quad (\text{A27})$$

Practically, we solve the fixed-point equations by first defining the following variables:

$$\begin{aligned}U &= \frac{\mu}{d^2} \sum_{k'} p_{k'} k' M_{k'}, \\ S &= \sqrt{\frac{\sigma^2}{d^2} \sum_{k'} p_{k'} k' q_{k'}}, \\ T &= \frac{\gamma \sigma^2}{d^2} \sum_{k'} p_{k'} k' \chi_{k'},\end{aligned}\quad (\text{A28})$$

and then by using Eq. (A23) to write the following set of equations in U , S , and T :

$$\begin{aligned}U &= \frac{\mu}{d^2} \sum_{k'} \frac{p_{k'} (k')^{\frac{3}{2}} S}{1 - T k'} w_1 \left(\frac{1 + U k'}{S \sqrt{k'}} \right), \\ 1 &= \frac{\sigma^2}{d^2} \sum_{k'} \frac{p_{k'} (k')^2}{(1 - T k')^2} w_2 \left(\frac{1 + U k'}{S \sqrt{k'}} \right), \\ T &= \frac{\gamma \sigma^2}{d^2} \sum_{k'} \frac{p_{k'} k'}{1 - T k'} w_0 \left(\frac{1 + U k'}{S \sqrt{k'}} \right).\end{aligned}\quad (\text{A29})$$

This reduces the original $3N$ fixed-point equations down to just three. These three equations are then solved using `scipy.optimize.root` in python, with an initial guess U, S, T either determined by a previously found solution with similar values of the parameters μ, σ, γ, p_k , or by running the GLV dynamics themselves for small N about 50 times to obtain empirical estimates for ϕ_k, M_k , and q_k . We then use the relation (derived from the fixed-point equations) $\chi_k = M_k \phi_k w_1(w_0^{-1}(\phi_k)) / \sqrt{\sigma^2 k} \sum_{k'} p_{k'} k' q_{k'} / d^2$ to determine a sensible initial guess for χ_k , which in turn gives initial guesses for U, S , and T . Here, w_0^{-1} is the inverse function of w_0 .

From U, S , and T , we can recover χ_k, M_k , and q_k using Eqs. (A23).

2. The abundance distribution

The abundance distribution $\text{AD}_k(x)$ for species with degree k in the original community is derived from Eq. (A21). It has the general form $\text{AD}_k(x) = (1 - \phi_k) \delta(x) + \Theta(x) P_{m_k, \Sigma_k}(x)$, where $\Theta(x) = 1$ if $x > 0$ and is zero otherwise. $P_{m_k, \Sigma_k}(x)$ is a Gaussian probability density function (PDF) with mean m_k and variance Σ_k^2 , Σ_k is defined in Eqs. (A24), and m_k is given by the following expression:

$$m_k = \frac{1 + \mu k \sum_{k'} p_{k'} k' M_{k'} / d^2}{1 - \gamma \sigma^2 k \sum_{k'} p_{k'} k' \chi_{k'} / d^2}. \quad (\text{A30})$$

The community-wide abundance distribution $\text{AD}(x)$, such as the one plotted in Fig. 2 in the main text, is equal to the weighted average of the individual degree distributions: $\text{AD}(x) = \sum_k p_k \text{AD}_k(x)$.

APPENDIX B: TREND OF ϕ_k AND M_{k^*} WITH DEGREE

In the main text, we claim that, for $\mu < 0$, the survival rate ϕ_k is always a decreasing function of the degree k , and that the same is true for a wide range of parameters for M_k . In this section we justify these claims.

1. Trend of ϕ_k with k

By definition, we can express the survival probability for species with degree k in the original community as [see Eqs. (A23)]

$$\phi_k = w_0(\Delta_k), \quad (\text{B1})$$

where Δ_k is defined in Eqs. (A24). The function w_0 is an increasing function of its argument. Hence, ϕ_k is an increasing (decreasing) function of k precisely when Δ_k is an increasing (decreasing) function of k . For fixed model parameters, Δ_k

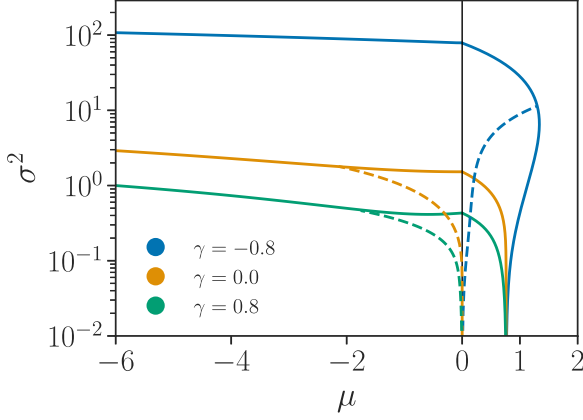


FIG. 7. Curves for which M_{k^*} and k^* are uncorrelated (dashed lines). To the left of the dashed lines, M_{k^*} and k^* are negatively correlated, and to the right of the dashed lines M_{k^*} and k^* are positively correlated. The area underneath the solid curves is stable, and the area above is unstable (see Fig. 1 in the main text for more detail).

has the following functional dependence on the degree k :

$$\Delta_k = \frac{1}{S} \left(\frac{1}{\sqrt{k}} + U \sqrt{k} \right), \quad (\text{B2})$$

where S and U are defined in Eqs. (A28), and they do not depend on k explicitly.

Differentiating Eq. (B2) with respect to k , we find that Δ_k is stationary in k when

$$k = \frac{1}{U}. \quad (\text{B3})$$

If $\mu < 0$, then $U < 0$ also, and the LHS and RHS have opposite signs (all other components in the equation are positive by definition), so there is no stationary point. Hence, ϕ_k is a decreasing function of k . If, on the other hand, μ is positive, then ϕ_k is decreasing provided the LHS is smaller than the RHS; if the LHS is larger, then the trend reverses. This becomes increasingly likely for more positive μ and larger abundances M_k .

2. Trend of M_{k^*} with k^*

We can follow the same procedure as for ϕ_k to find the degree at which the abundance M_k has a stationary point. It is stationary when

$$k = \frac{\phi_k - M_k}{U \phi_k + T M_k}, \quad (\text{B4})$$

where T is defined in Eqs. (A28). This condition is not as straightforward to analyze as the equivalent condition for the stationary point of ϕ_k in Eq. (B3). However, we can still find the general trend of M_{k^*} with k^* by noting (as we do in the main text) that the covariance $\text{Cov}(M_{k^*}, k^*) = (\sum_{k^*} p_{k^*} M_{k^*} k^*) - (\sum_{k^*} p_{k^*} M_{k^*})(\sum_{k^*} p_{k^*} k^*)$ is negative whenever M_{k^*} is a decreasing function of k^* . In Fig. 7, we plot the curve satisfying $\text{Cov}(M_{k^*}, k^*) = 0$ in the (μ, σ^2) plane for different values of γ and fixed network structure. Demonstrating that when $\mu < 0$, only a small range of parameters in the stable phase give rise to positive

correlations (right of the curve), hence our focus on this trend in particular in the main text.

APPENDIX C: STABILITY

1. Diverging abundances

To numerically find the boundary between the fixed point and the point at which the average abundance M diverges, we first express the fixed-point equations (A23) in terms of the new variables $\chi_k, \tilde{M}_k = M_k / \sqrt{\sum_{k'} p_{k'} q_{k'}}$, and $\tilde{q}_k = q_k / \sum_{k'} p_{k'} q_{k'}$. Unlike M_k and q_k , \tilde{M}_k and \tilde{q}_k remain finite when the average abundance diverges. In the limit of infinite average abundance, the new fixed-point equations are equivalent to Eqs. (A23) with the replacements $M_k \rightarrow \tilde{M}_k, q_k \rightarrow \tilde{q}_k$, and $\Delta_k \rightarrow \tilde{\Delta}_k$, where

$$\tilde{\Delta}_k = \frac{\mu k \sum_{k'} p_{k'} k' \tilde{M}_{k'} / d^2}{\sigma \sqrt{k} \sum_{k'} p_{k'} k' \tilde{q}_{k'} / d}. \quad (\text{C1})$$

Solving these new fixed-point equations, together with the condition $\sum_k \tilde{q}_k = 1$, gives the diverging abundance curves in Fig. 1 in the main text.

2. Linear instability

To derive stability condition (7) from the main text, we consider a linear perturbation to the effective dynamics in Eq. (A19) near a fixed point. We follow along the lines of the stability analyses in Refs. [32,52] (see also Ref. [44] for a derivation involving block structured interactions, which generalizes the present argument).

The local stability of possible fixed points can be probed by addition of an infinitesimal independent and identically distributed Gaussian perturbation $\epsilon \xi_k(t)$ to each equation in the effective dynamics in Eq. (A19). In the stable regime, we expect the system to return to the fixed point when perturbed; that is, we expect the response of the system to the perturbation to decay to zero as $t \rightarrow \infty$.

Adding the perturbation $\epsilon \xi_k(t)$ to the effective dynamics [Eq. (A19)], we have

$$\begin{aligned} \dot{x}_k(t) = & x_k(t) \left(1 - x_k(t) + \frac{\mu k}{d^2} \sum_{k'} p_{k'} k' M_{k'}(t) + \frac{\gamma \sigma^2 k}{d^2} \right. \\ & \times \left. \sum_{k'} p_{k'} k' \int dt G_{k'}(t, t') x_{k'}(t') + \eta_k(t) + \epsilon \xi_k(t) \right), \end{aligned} \quad (\text{C2})$$

where $M_k(t)$, $G_k(t)$, and the noise term $\eta_k(t)$ are defined in Eqs. (A20).

We quantify the linear response of $x_k(t)$ and $\eta_k(t)$ to the perturbation $\epsilon \xi(t)$ about the fixed point by $y_k(t)$ and $\zeta_k(t)$, respectively, so that

$$\begin{aligned} x_k(t) &= x_k^* + \epsilon y_k(t), \\ \eta_k(t) &= \eta_k^* + \epsilon \zeta_k(t). \end{aligned} \quad (\text{C3})$$

From this, we can self-consistently relate the responses to each other using Eqs. (A20)

$$\langle \zeta^a(t) \zeta^a(t') \rangle = \frac{\sigma^2 k}{d^2} \sum_{k'} p_{k'} k' \langle y_k(t) y_{k'}(t') \rangle. \quad (\text{C4})$$

Assuming time translation invariance of the fixed point in the long-time limit, we obtain the following equation for the time dependence of the perturbed abundances:

$$\dot{y}_k(t) = x_k^* \left(-y_k(t) + \frac{\gamma \sigma^2 k}{d^2} \sum_{k'} p_{k'} k' \int_0^t dt' G_k(t-t') y_k(t') + \zeta_k(t) + \xi_k(t) \right). \quad (\text{C5})$$

We now follow Refs. [32,52] by taking the Fourier transform (denoted with a hat, which we note is not related to the hatted variables in the generating functional calculations in Appendix A)

$$i\omega \hat{y}_k(\omega) = x_k^* \left(-\hat{y}_k(\omega) + \frac{\gamma \sigma^2 k}{d^2} \sum_{k'} p_{k'} k' \hat{G}_k(\omega) \hat{y}_k(\omega) + \hat{\zeta}_k(\omega) + \hat{\xi}_k(\omega) \right). \quad (\text{C6})$$

Squaring and averaging over the distribution of the perturbing noise ξ_k ,

$$\left\{ \frac{|\omega|^2}{(x_k^*)^2} + \left| 1 - \frac{\gamma \sigma^2 k}{d^2} \sum_{k'} p_{k'} k' \hat{G}_k(\omega) \right|^2 \right\} \langle |\hat{y}_k(\omega)|^2 \rangle_\xi = \phi_k \left\{ \frac{\sigma^2 k}{d^2} \sum_{k'} p_{k'} k' \langle |\hat{y}_{k'}(\omega)|^2 \rangle_\xi + 1 \right\}, \quad (\text{C7})$$

where the factor of the survival rate ϕ_k is due to the fact that Eq. (C5) only applies to nonzero fixed points. Fluctuations around the zero point decay and hence do not contribute to $\langle |\hat{y}_k(\omega)|^2 \rangle$. Noticing that $\hat{G}_k(0) = \chi^a$, we now set $\omega = 0$ (see Ref. [52]) and find

$$\left\{ 1 - \frac{\gamma \sigma^2 k}{d^2} \sum_{k'} p_{k'} k' \chi_{k'} \right\}^2 Y_k = \phi_k \left\{ \frac{\sigma^2 k}{d^2} \sum_{k'} p_{k'} k' Y_{k'} + 1 \right\}, \quad (\text{C8})$$

where $Y_k \equiv \langle |\hat{y}_k(0)|^2 \rangle$. Assuming a stationary state in which $\langle y_k(t) y_k(t+\tau) \rangle$ depends on τ only, then $Y_k = \int d\tau \langle y_k(t) y_k(t+\tau) \rangle$. In the stable regime, $y_k(t) \rightarrow 0$ as $t \rightarrow 0$, and therefore Y_k is finite. Hence, if Y_k is not finite, then this signals the onset of linear instability. Hence, the onset of linear instability corresponds to the point at which the only solution to Eq. (C8) for which Y_k diverges for some degree k .

Equation (C8) is equivalent to the condition for linear (in)stability given in the main text [Eq. (7)]. To make the connection, we first use the fixed-point equations (A23) (the one for χ_k) to rearrange Eq. (C8) into the following form:

$$\tilde{Y}_k = \frac{\sigma^2 k \chi_k^2}{d^2 \phi_k} \sum_{k'} p_{k'} \left[k' + \frac{1}{\sum_{k''} p_{k''} Y_{k''}} \right] \tilde{Y}_{k'}, \quad (\text{C9})$$

where we have defined $\tilde{Y}_k = Y_k / (\sum_{k'} p_{k'} Y_{k'})$, which remains finite, even if Y_k diverges for some k . At the point of linear instability, the quantity $1 / (\sum_{k'} p_{k'} Y_{k'}) = 0$, and Eq. (C9) is

an eigenvalue equation

$$Y_k = \sum_{k'} S_{kk'} Y_{k'}, \quad (\text{C10})$$

where \mathbf{S} is a matrix with kk' element equal to $S_{kk'} = \sigma^2 k \chi_k^2 p_{k'} k' / (d^2 \phi_k)$. All elements of the matrix \mathbf{S} are positive, as are all elements of the vector \mathbf{Y} (by definition of Y_k). Hence, \mathbf{Y} is the Perron-Frobenius (PF) eigenvector of \mathbf{S} , with PF eigenvalue equal to 1. Furthermore, as \mathbf{S} can be written as the outer product of two vectors [$\mathbf{S} = \mathbf{a} \mathbf{b}^T$, for $a_k = \sigma^2 k \chi_k^2 / (d^2 \phi_k)$ and $b_k = p_k k$], its PF eigenvalue is given by the inner product of these two vectors ($\mathbf{a}^T \mathbf{b} = \sum_k \mathbf{a}_k \mathbf{b}_k$). That is, the linear instability occurs at the point when

$$\frac{\sigma^2}{d^2} \sum_k p_k \frac{k^2 \chi_k^2}{\phi_k} = 1. \quad (\text{C11})$$

To see that the LHS is smaller than 1 in the stable regime, we repeat the same argument, but we write $Y = \sum_k p_k Y_k$ in Eq. (C9) and do not assume that Y diverges. This time, the eigenvalue condition is different; we have $\lambda_{\text{PF}}[\mathbf{S} + \mathbf{p}/\mathbf{Y}] = 1$, where we have defined the matrix \mathbf{p} with elements $p_{kk'} = \sigma^2 \chi_k^2 p_{k'} / (d^2 \phi_k)$. All elements of the matrix \mathbf{p} are positive. It is known that the PF eigenvalue of a matrix is an increasing function of its elements [70,71]. Hence, we have $\lambda_{\text{PF}}[\mathbf{S}] \leq \lambda_{\text{PF}}[\mathbf{S} + \mathbf{p}/\mathbf{Y}] = 1$ in the stable regime. That is, in the stable regime, the LHS of Eq. (C11) is less than 1.

In Fig. 1 in the main text, we solve for the boundary of the linearly stable region in parameter space by adding the condition in Eq. (C11) to the fixed-point equations.

APPENDIX D: INTERACTION STATISTICS IN THE SURVIVING COMMUNITY

To find the quantities defined in Eq. (10), we employ a similar philosophy to that used in Ref. [37], except here we use a cavity approach. In this case, the cavity approach helps to elucidate the mechanism behind the trends seen in Fig. 6 by revealing the origins of all the contributing factors to the quantities in Eq. (10).

1. The cavity approach

At the fixed point, we must have that

$$x_i = \max \left(0, 1 + \sum_j A_{ij} \alpha_{ij} x_j + h_i \right), \quad (\text{D1})$$

where h_i is again an external field that we include for analytical purposes, and which we later set to zero.

Let us suppose that we introduce a new "cavity" species, which we endow with index 0, to the network. We suppose that the cavity species has degree k (in the original community). Let us now inspect the following quantity:

$$\mu_0^{(k)} = \sum_j A_{0j} \alpha_{0j} \theta_j, \quad (\text{D2})$$

where $\theta_j(x_j) = 0$ if a species is extinct and $\theta_j(x_j) = 1$ if the species survives. Following the usual procedure for cavity calculations, we attempt to find θ_j in terms of system parameters

before the addition of the cavity species. We write

$$\theta_j = \theta_j^{(0)} + \delta\theta_j, \quad (\text{D3})$$

so that $\delta\theta_j$ (which takes values 0 or ± 1) accounts for the changes in the numbers of surviving species due to the introduction of the cavity species. We expect the number of species that go extinct due to the introduction of the new species to be small.

Inserting this into Eq. (D2) and defining $\alpha_{ij} = \mu/d + a_{ij}$, we find

$$\mu_0^{(k)} = \frac{\mu}{d} \sum_j A_{0j} \theta_j + \sum_j A_{0j} a_{0j} \theta_j^{(0)} + \sum_j A_{0j} \alpha_{0j} \delta\theta_j. \quad (\text{D4})$$

Let us now use the fact that we have many species to write each of these terms in terms of the statistics of the community.

2. Averaging Eq. (D4) over the wider pool of species

Let us now discuss the statistics of each of the terms in Eq. (D4), keeping the cavity interactions A_{0j} , α_{0j} , and α_{j0} fixed. Specifically, we first take the mean with respect to the interactions α_{ij} and the network A_{ij} , where both i and j are not equal to zero, and then discuss the variance with respect to these same quantities. We denote the average with respect to these variables as $\langle \cdot \rangle_0$ (as opposed to $\langle \cdot \rangle$, which indicates an average over all interaction coefficients, including those of the cavity species).

We treat the average over the random variables A_{0j} , α_{0j} , A_{j0} , and α_{j0} separately so that we can better see how $\mu_0^{(k)}$ relates to other random quantities of interest, for example, the abundance x_0 . This will help us to understand the origin of the behavior of $\mu_k^{(0)}$ as k is varied (shown in Fig. 6).

Taking, for example, the first term in Eq. (D4), we first examine its mean, and then its fluctuations. We find that

$$\frac{\mu}{d} \left\langle \sum_j A_{0j} \theta_j \right\rangle_0 = \frac{\mu}{d} \sum_j A_{0j} [\langle \theta_j^{(0)} \rangle_0 + \langle \delta\theta_j \rangle_0], \quad (\text{D5})$$

where we have used that the survival of species before the introduction of the cavity is independent of A_{0j} . We can rewrite the second of these terms using the fact that

$$\langle \delta\theta_j \rangle_0 = \frac{d\phi_{kj}}{dh} A_{j0} \alpha_{j0} x_0, \quad (\text{D6})$$

where we write k_j for the degree of species j , and we obtain

$$\frac{\mu}{d} \left\langle \sum_j A_{0j} \theta_j \right\rangle_0 = \frac{\mu}{d} \sum_j A_{0j} \left[\phi_{kj} + \frac{d\phi_{kj}}{dh} \alpha_{j0} x_0 \right]. \quad (\text{D7})$$

We see that the second of these terms is a small $O(1/N)$ correction compared to the first, and hence we can ignore it. We now average over both the interaction statistics of the original community and the cavity species to obtain

$$\frac{\mu}{d} \left\langle \sum_j A_{0j} \theta_j \right\rangle \approx \frac{\mu}{d} \sum_{k'} \frac{k k'}{dN} \sum_{j \in S_{k'}} \langle \theta_j^{(0)} \rangle_0 = \frac{k}{d^2} \sum_{k'} k' p_{k'} \phi_{k'}, \quad (\text{D8})$$

where we write $S_{k'}$ for the set of species with degree k' , and we have used that the degree distribution of the network can be written $p_k = N_k/N$ when $N \rightarrow \infty$, where N_k is the number

of species with degree k . We hence see that the mean of the first term in Eq. (D4) is nonvanishing in the thermodynamic limit.

Let us now examine the fluctuations of this same term [the first in Eq. (D4)]. One can see immediately from the approach in Appendix A that the generating functional for the ensemble of all species factorizes in the limit $N \rightarrow \infty$. This means that the variance of (or correlations between) any order parameters such as ϕ_k or M_k are subleading in $1/N$ in the thermodynamic limit. So, keeping A_{0j} and α_{0j} fixed, we see that fluctuations due to randomness in the wider community without the cavity species can always be neglected. Let us now examine the fluctuations of $\mu d^{-1} \sum_j A_{0j} \theta_j$ due to fluctuations in the interactions of the cavity species. Since the probability that each link in the network is independent of the rest of the links in the network, we have

$$\text{Var} \left[\frac{\mu}{d} \sum_j A_{0j} \theta_j \right] \approx \frac{\mu^2}{d^2} \sum_j [\langle A_{0j} \rangle - \langle A_{0j} \rangle^2] \phi_{k_j}^2, \quad (\text{D9})$$

which is subleading in $1/d \sim 1/N$. So, we see that the first term in Eq. (D4) can be approximated by its mean in Eq. (D8).

Let us now turn our attention to the third term in Eq. (D4). We will see that, in contrast to the first term, this term has non-vanishing fluctuations. We once again examine the ensemble average of this term (keeping the interaction coefficients with the cavity species fixed), noting again that the fluctuations of the order parameters of the wider community can be ignored. Using Eq. (D6), we find

$$\begin{aligned} \left\langle \sum_j A_{0j} \alpha_{0j} d\theta_j \right\rangle_0 &= \sum_j A_{0j} \alpha_{0j} \langle d\theta_j \rangle_0 \\ &= x_0 \sum_j A_{0j} \alpha_{0j} \frac{d\phi_{kj}}{dh} \alpha_{j0}, \end{aligned} \quad (\text{D10})$$

where we have used the fact that $A_{0j} = A_{j0}$.

The expression obtained in Eq. (D10) differs depending on the precise values of the interaction coefficients of the cavity species [noting that x_0 also depends on these quantities through Eq. (D1)]. However, we can demonstrate that the sum over j in Eq. (D10) is a self-averaging quantity that can be replaced by its mean, meaning that all the relevant variation in the third term in Eq. (D4) can be captured by x_0 , multiplied by a constant factor.

That is, we have

$$\begin{aligned} \left\langle \sum_j A_{0j} \alpha_{0j} \frac{d\phi_{kj}}{dh} \alpha_{j0} \right\rangle &= \frac{k \gamma \sigma^2}{d^2} \sum_{k'} k' p_{k'} \frac{d\phi_{k'}}{dh}, \\ \text{Var} \left[\sum_j A_{0j} \alpha_{0j} \frac{d\phi_{kj}}{dh} \alpha_{j0} \right] &= \sum_j [\langle A_{0j} \rangle \langle (\alpha_{0j} \alpha_{j0})^2 \rangle \\ &\quad - \langle A_{0j} \rangle^2 \langle \alpha_{0j} \alpha_{j0} \rangle^2] \left[\frac{d\phi_{kj}}{dh} \right]^2. \end{aligned} \quad (\text{D11})$$

We see once again that the fluctuations of this quantity vanish in the thermodynamic limit. We can thus approximate the sum $\sum_j A_{0j} \alpha_{0j} \frac{d\phi_{kj}}{dh} \alpha_{j0}$ by its average. The third term in Eq. (D4) is thus well approximated by

$$\sum_j A_{0j} \alpha_{0j} \delta\theta_j \approx x_0 \frac{k\gamma\sigma^2}{d^2} \sum_{k'} k' p_{k'} \frac{d\phi_{k'}}{dh}, \quad (\text{D12})$$

where we see that the randomness is all accounted for by the variable x_0 . In a certain sense, we were "lucky" that we could encapsulate the relevant fluctuations of the third term in Eq. (D4) entirely in the random variable x_0 . The second term in Eq. (D4) is more complicated. To understand why, we compare with the cavity calculation that could have been

performed to obtain the results in Eqs. (3) and (4) (instead of the generating functional approach of Appendix A).

3. Lemma: Relating the random variable z in Eq. (3) to the interaction coefficients

The fixed points of Eq. (1) satisfy

$$x_i \left(1 - x_i + \sum_j A_{ij} \alpha_{ij} x_j + h_i \right) = 0. \quad (\text{D13})$$

Introducing a new species 0 as a "cavity," one finds

$$x_j \approx x_j^{(0)} + \frac{dx_j}{dh_j} A_{j0} \alpha_{j0} x_0. \quad (\text{D14})$$

One thus arrives at

$$x_0 \left(1 - x_0 + \frac{\mu}{d} \sum_j A_{0j} x_j^{(0)} + \sum_j A_{0j} a_{0j} x_j^{(0)} + x_0 \sum_j A_{0j} \alpha_{0j} \alpha_{j0} \frac{dx_j}{dh_j} \right) = 0, \quad (\text{D15})$$

and consequently

$$x_0 = \max \left(0, \frac{1 + \frac{\mu}{d} \sum_j A_{0j} x_j^{(0)} + \sum_j A_{0j} a_{0j} x_j^{(0)} + h_j}{1 - \sum_j A_{0j} \alpha_{0j} \alpha_{j0} \frac{dx_j}{dh_j}} \right). \quad (\text{D16})$$

Supposing that species 0 has original degree k , we can compare to Eq. (3), and we see that the term $\sum_j A_{0j} a_{0j} x_j^{(0)}$ in the expression above corresponds to a Gaussian random variable, i.e.,

$$\sum_j A_{0j} a_{0j} x_j^{(0)} = z\sigma \sqrt{\frac{k}{d} \sum_{k'} \frac{k' p_{k'}}{d} q_{k'}}, \quad (\text{D17})$$

where z is a zero-mean, unit-variance Gaussian random variable, as in Eq. (3). One notes that we can also deduce this from the cavity approach simply by computing the mean and the variance of $\sum_j A_{0j} a_{0j} x_j^{(0)}$. The variance is given as follows:

$$V_x \equiv \left\langle \sum_j A_{0j} a_{0j} x_j^{(0)} \sum_{j'} A_{0j'} a_{0j'} x_{j'}^{(0)} \right\rangle = \left\langle \sum_{jj'} \delta_{jj'} \frac{\sigma^2}{d} A_{0j} [x_j^{(0)}]^2 \right\rangle \approx \frac{\sigma^2 k}{d^2} \sum_{k'} k' p_{k'} q_{k'}. \quad (\text{D18})$$

The second term in Eq. (D4) (i.e., $\sum_j A_{0j} a_{0j} \theta_j^{(0)}$) has a similar structure to the term $\sum_j A_{0j} a_{0j} x_j^{(0)}$. We see that it too must be a Gaussian random variable, with some correlation with the random variable z that appears in Eq. (3) (given that it is also dependent on the same random variables a_{0j}). If we can find the variance of $\sum_j A_{0j} a_{0j} \theta_j^{(0)}$ and its correlation with z , then we will understand fully how to relate $\mu_0^{(k)}$ to the fixed-point quantities in Eq. (4), given that we already have the approximations for the first and third terms in Eq. (D4) in Eqs. (D8) and (D12), respectively.

4. Relating the fluctuating part of Eq. (D4) to the fluctuating part of Eq. (3)

Let us now compute the variance of the quantity $\sum_j A_{0j} a_{0j} \theta_j^0$ in Eq. (D4). We find

$$V_\theta \equiv \left\langle \sum_j A_{0j} a_{0j} \theta_j^{(0)} \sum_{j'} A_{0j'} a_{0j'} \theta_{j'}^{(0)} \right\rangle = \left\langle \sum_{jj'} \delta_{jj'} \frac{\sigma^2}{d} A_{0j} [\theta_j^{(0)}]^2 \right\rangle = \frac{\sigma^2 k}{d^2} \sum_{k'} k' p_{k'} \phi_{k'}. \quad (\text{D19})$$

We can thus think of the second term in Eq. (D4) as also being a zero-mean Gaussian random variable, so we write

$$\sum_j A_{0j} a_{0j} \theta_j^0 \equiv y\sqrt{V_\theta}, \quad (\text{D20})$$

where y is a Gaussian random variable with unit variance. Let us now understand how y is related to z in Eq. (D17) by finding the covariance,

$$C_{x\theta} \equiv \left\langle \sum_j A_{0j} a_{0j} \theta_j^{(0)} \sum_{j'} A_{0j'} a_{0j'} x_{j'}^{(0)} \right\rangle = \left\langle \sum_{jj'} \delta_{jj'} \frac{\sigma^2}{d} A_{0j} \theta_j^{(0)} x_j^{(0)} \right\rangle = \frac{\sigma^2 k}{d^2} \sum_{k'} k' p_{k'} M_{k'}. \quad (\text{D21})$$

We can thus write

$$y = \frac{C_{x\theta}}{\sqrt{V_x V_\theta}} z + z' \sqrt{1 - \frac{C_{x\theta}}{\sqrt{V_x V_\theta}}}, \quad (\text{D22})$$

where z' is a zero-mean unit-variance Gaussian random variable that is independent of z . We are now in a position to write Eq. (D4) entirely in terms of the statistics of the surviving community.

5. Incoming and outgoing statistics of nodes with given degree

Now, inserting Eqs. (D8), (D12), (D20), and (D22) into Eq. (D4), we obtain

$$\mu_0^{(k)} = \frac{\mu k}{d^2} \sum_{k'} k' p_{k'} \phi_{k'} + z_k \frac{\sigma \sqrt{k}}{d} \frac{\sum_{k'} k' p_{k'} M_{k'}}{\sqrt{\sum_{k'} k' p_{k'} q_{k'}}} + C_{z'} z' + x_k(z_k) \frac{\gamma \sigma^2 k}{d^2} \sum_{k'} k' p_{k'} \frac{d\phi_{k'}}{dh}, \quad (\text{D23})$$

where we have now evaluated some terms explicitly to highlight their dependence on k , and we simply write $C_{z'}$ for the coefficient multiplying z' , since this will not affect the quantities in which we are interested.

Let us now consider the following quantity,

$$v_0^{(k)} = \sum_j A_{j0} \alpha_{j0} \theta_j, \quad (\text{D24})$$

which instead tells us about the outgoing links of a node with degree k . We can perform exactly the same manipulations as we did for $\mu_0^{(k)}$ to arrive at

$$v_0^{(k)} = \frac{\mu k}{d^2} \sum_{k'} k' p_{k'} \phi_{k'} + z_k \frac{\gamma \sigma \sqrt{k}}{d} \frac{\sum_{k'} k' p_{k'} M_{k'}}{\sqrt{\sum_{k'} k' p_{k'} q_{k'}}} + C_{z'} z' + x_k(z_k) \frac{\sigma^2 k}{d^2} \sum_{k'} k' p_{k'} \frac{d\phi_{k'}}{dh}. \quad (\text{D25})$$

We notice the symmetry between the expressions in Eqs. (D23) and (D25). What was an effect of the neighbors of a node on the node itself in Eq. (D23) becomes the effect of the node on its neighbors in Eq. (D25). This is why we see factors of γ multiplying complementary terms in the two expressions.

Now, to obtain the ensemble average of the above expressions, we simply average over realizations of the variable z_k , conditioning on the survival of the cavity species 0. This means that we require $x_k(z_k) > 0$, which in turn requires that

$$z_k > -\Delta_k(h) \equiv -\frac{1 + \mu k \sum_{k'} p_{k'} k' M_{k'} / d^2 + h}{\sigma \sqrt{k} \sum_{k'} p_{k'} k' q_{k'} / d}. \quad (\text{D26})$$

The probability of survival is given by

$$\phi_k = \int_{-\Delta_k}^{\infty} dz \frac{1}{\sqrt{2\pi}} e^{-z^2/2}. \quad (\text{D27})$$

Hence, averaging over the variable z_k in Eqs. (D23) and (D25), we obtain

$$\begin{aligned} \frac{\mu_k^{\text{in}}}{d^*} &\equiv \frac{\langle \mu_0^{(k)} \theta_0 \rangle}{kr} = \frac{\mu}{d} + \frac{\sigma^2}{d} \frac{d\phi_k}{dh} \frac{\sum_{k'} k' p_{k'} M_{k'}}{\sum_{k'} k' p_{k'} \phi_{k'}} \\ &\quad + \frac{\gamma \sigma^2}{d} M_k \frac{\sum_{k'} k' p_{k'} \frac{d\phi_{k'}}{dh}}{\sum_{k'} k' p_{k'} \phi_{k'}}, \\ \frac{\mu_k^{\text{out}}}{d^*} &\equiv \frac{\langle v_0^{(k)} \theta_0 \rangle}{kr} = \frac{\mu}{d} + \frac{\gamma \sigma^2}{d} \frac{d\phi_k}{dh} \frac{\sum_{k'} k' p_{k'} M_{k'}}{\sum_{k'} k' p_{k'} \phi_{k'}} \\ &\quad + \frac{\sigma^2}{d} M_k \frac{\sum_{k'} k' p_{k'} \frac{d\phi_{k'}}{dh}}{\sum_{k'} k' p_{k'} \phi_{k'}}, \end{aligned} \quad (\text{D28})$$

where here we have used the fact that

$$\int_{-\Delta}^{\infty} dz e^{-z^2/2} z = \frac{1}{\sqrt{2\pi}} e^{-\Delta^2/2} = \frac{d\phi_k}{dh} \sqrt{\sigma^2 \frac{k}{d^2} \sum_{k'} p_{k'} k' q_{k'}}, \quad (\text{D29})$$

and we recall the definitions of r from the main text:

$$r = \frac{\sum_k p_k \phi_k k}{\sum_k p_k}. \quad (\text{D30})$$

To express the incoming and outgoing interaction strengths in Eqs. (D28) in terms of the degree in the surviving community k^* (rather than the degree in the initial community k), we use the correspondence $E[k^* | k] = rk$ (see Sec. IV A for a discussion and Appendix E for mathematical details), as well as the fact that the expected degrees in the surviving community are concentrated around their mean value. Hence, if we treat k as a continuous variable, we can approximate $k^* = rk$ to leading order in $1/d$.

Practically, the curves in Fig. 6 are produced by plotting μ_k^{in}/d^* in Eqs. (D28) against k/r . This is equivalent to plotting μ_k^{in}/d^* against k^* .

6. Interpretation of the trends in Fig. 6

Let us now consider how the cavity approach that we have taken can help us to understand the trends in Fig. 6. This is accomplished by interpreting physically each of the terms in Eqs. (D23) and (D25), with the help of Eq. (D4).

Equation (D23) describes the sum of incoming interactions to a node of original degree k as a random variable. The first term in this expression is deterministic, and is simply the mean interaction, weighted by the number of surviving neighbors (which will depend on k). The second and third terms encode the fluctuations in the weights of the neighbors' interactions. However, we note that once we average over the disorder (conditioning on survival of species 0), the term proportional to z' vanishes, and the Gaussian distribution of z_k is truncated. That is, only species with sufficiently favorable interactions survive, and this biases the mean interaction of surviving species towards higher values. Finally, the last term encapsulates the fact the survival of the neighbors of a species is dependent on the abundance of that species. In turn, the survival of the neighboring species affects the statistics of the incoming interactions (i.e., the abundance of a species affects its own incoming interactions via its effect on its neighbors). We note that this last effect depends on the correlation between the incoming and outgoing links.

In the case where $\gamma = 0$ [i.e., there is no correlation between the incoming interactions to a species and outgoing effect of a species on its neighbors, as is the case in Fig. 6(b)], the final term mentioned above does not contribute. Instead, only the direct influence of a species' neighbors is relevant. Since we condition on the survival of the species with degree k , the incoming interactions cannot be too negative. This is encapsulated by the lower limit imposed on the truncated Gaussian random variable z_k in Eq. (D23). For small k , this lower limit is effectively $-\infty$, which is reflected in the survival of nearly all species with small degree (i.e., $\phi_k \approx 1$ for small k ; see Fig. 5). This means that the term involving z_k averages to nil when we integrate over all its possible values, and we find that species with low degree have interactions that are the same as the original community. However, as we increase k , ϕ_k decreases, and the lower limit on the integration of z_k increases also. This means that a bias is introduced, whereby only species with more favorable incoming interactions survive. This explains the upwards trend in Fig. 6(b) for the incoming interactions.

Likewise, we can interpret each of the terms in Eq. (D25) as follows: The first is again simply the mean interaction, weighted by the number of surviving neighbors. The second and third terms now reflect that each outgoing interaction from a node can fluctuate, but these outgoing interactions correlate with the incoming interactions. For this reason, the outgoing interactions can once again be related to the variable z_k , and thus the survival probability of the species with original degree k . Since we condition on this survival, this biases the outgoing interactions so that the incoming interactions are favorable (note that the resulting effect on the outgoing interactions then depends on the sign of γ). Finally, the last term again encapsulates the fact that whether or not the neighbors of a species survive is dependent on the abundance of that species. Since we only look at the outgoing interactions from

a species (with degree k) to species that survive, if the abundance of the species with degree k is higher, its influence on the survival of the surrounding species is greater. For greater abundances, a greater number of species can be killed, and the correction to the average outgoing interaction is greater. Since M_k reduces with increasing k , we see that the effect of this term is greatest for small k , and it reduces to nil for large k . This explains the downwards trend in the outgoing interactions in Fig. 6(b).

The case of $\gamma = 0$ in Fig. 6(b) is useful, because it separates the dependence of the outgoing and incoming interactions. We see that by varying γ , we simply obtain a superposition of the aforementioned effects. For example, when $\gamma = 1$, the outgoing and incoming interactions must be the same. Hence, $\mu_k^{\text{out}} = \mu_k^{\text{in}}$ and the corresponding curve in Fig. 6(a) is seen to be a kind of "average" of the upwards and the downwards trends. On the other hand, for $\gamma = -1$, we see that the fluctuations in the incoming and outgoing interactions are exactly the negative of each other, hence the kind of mirror-image effect in Fig. 6(c).

APPENDIX E: STRUCTURE OF THE SURVIVING NETWORK

1. Probability that species with degree k and k' interact in the surviving community

To find the statistics of the adjacency matrix in the surviving community, we follow a strategy employed in Ref. [37] that was used to find the statistics of the surviving interaction matrix α in the fully connected model. Consider the following modification of the generating functional in Appendix A, which includes an additional term proportional to the interaction matrix in the surviving community:

$$Z[\lambda] = \int \mathcal{D}\mathbf{x} \mathcal{D}\hat{\mathbf{x}} Z_0[\mathbf{x}, \hat{\mathbf{x}}, \boldsymbol{\psi} = \mathbf{0}] \exp \times \left[-i \sum_{ij} \int dt A_{ij} \alpha_{ij} \hat{x}_i(t) x_j(t) + i \sum_{ij} A_{ij} \int dt \lambda_{ij}(t) \theta_i(t) \theta_j(t) \right]. \quad (\text{E1})$$

The functional $Z_0[\mathbf{x}, \hat{\mathbf{x}}, \boldsymbol{\psi} = \mathbf{0}]$ is the remaining part of the generating functional which appears in Eq. (A1); it is not relevant to our arguments in this section. As in Appendix D, $\theta_i(t) = 1$ if the corresponding abundance $x_i(t) > 0$, and is zero otherwise. In other words, $\theta_i(t)$ is equal to 1 only if species i is alive at time t . The functions $\lambda_{ij}(t)$ are auxiliary fields which we will set to zero at the end of this derivation.

Taking a functional derivative of Z with respect to $\lambda_{ij}(t)$, then setting $\lambda_{ij}(t) = 0$, yields

$$\frac{\delta Z[\lambda]}{\delta \lambda_{ij}(t)} = i A_{ij} \theta_i(t) \theta_j(t). \quad (\text{E2})$$

We are interested in the average interactions between species with degree k and k' . Using Eq. (E2), we can relate this

quantity to the generating functional via

$$\begin{aligned} & \frac{1}{N_k^* N_{k'}^*} \sum_{i \in S_k^*} \sum_{j \in S_{k'}^*} \langle A_{ij} \theta_i^* \theta_j^* \rangle_{\mathbf{A}, \mathbf{A}} \\ &= -i \lim_{t \rightarrow \infty} \frac{1}{N_k^* N_{k'}^*} \sum_{i \in S_k^*} \sum_{j \in S_{k'}^*} \left\langle \frac{\delta Z[\boldsymbol{\lambda}]}{\delta \lambda_{ij}(t)} \right\rangle_{\mathbf{A}, \mathbf{A}_{\lambda=0}}. \end{aligned} \quad (\text{E3})$$

Averaging $Z[\boldsymbol{\lambda}]$ over \mathbf{A} , and proceeding similarly to the average calculated in Appendix A, we find

$$\begin{aligned} & \langle Z[\boldsymbol{\lambda}] \rangle_{\mathbf{A}, \alpha} \\ &= \int \mathcal{D}\mathbf{x} \mathcal{D}\widehat{\mathbf{x}} \mathcal{Z}_0[\mathbf{x}, \widehat{\mathbf{x}}, \boldsymbol{\psi} = 0] \exp \left[\frac{1}{2} \sum_{ij} \ln \left\{ 1 + \frac{k_i k_j}{dN} \right. \right. \\ & \quad \times \left(\langle e^{-i \int dt (\alpha \widehat{x}_i(t) x_j(t) + \beta \widehat{x}_j(t) x_i(t))} \rangle_{(\alpha, \beta)} \right) \\ & \quad \left. \left. \times e^{i \int dt (\lambda_{ij}(t) + \lambda_{ji}(t)) \theta_i(t) \theta_j(t)} - 1 \right\} \right], \end{aligned} \quad (\text{E4})$$

where, similarly to Appendix A, we have written $\alpha_{ij} \rightarrow \alpha$ and $\alpha_{ji} \rightarrow \beta$ because the joint distribution of $(\alpha_{ij}, \alpha_{ji})$ does not depend on the indices i, j . Differentiating Eq. (E4) with respect to $\lambda_{ij}(t)$ and setting $\lambda_{ij}(t) = 0$ gives

$$\begin{aligned} & \langle A_{ij} \theta_i(t) \theta_j(t) \rangle_{\mathbf{A}, \alpha} \\ &= \left\langle \frac{\frac{k_i k_j \theta_i(t) \theta_j(t)}{dN} \left(e^{-i \int dt (\alpha \widehat{x}_i(t) x_j(t) + \beta \widehat{x}_j(t) x_i(t))} \right)_{(\alpha, \beta)}}{1 + \frac{k_i k_j}{dN} \left(\langle e^{-i \int dt (\alpha \widehat{x}_i(t) x_j(t) + \beta \widehat{x}_j(t) x_i(t))} \rangle_{(\alpha, \beta)} - 1 \right)} \right\rangle_{\mathbf{A}, \alpha}. \end{aligned} \quad (\text{E5})$$

This expression simplifies greatly if the network is dense (where the average degree d is large), as it is in our model. From the statistics of the interactions α_{ij} in Eq. (2), we know that $\alpha_{ij} = O(d^{-1/2})$ and $\langle \alpha_{ij} \rangle_{\alpha} = O(d^{-1})$. Hence, to leading order in $1/d$, the statistics of the interactions do not directly contribute to Eq. (E5) and we have

$$\langle A_{ij} \theta_i(t) \theta_j(t) \rangle_{\mathbf{A}, \alpha} = \left\langle \frac{k_i k_j}{dN} \theta_i(t) \theta_j(t) \right\rangle_{\mathbf{A}, \alpha} + O(d^{-1}). \quad (\text{E6})$$

Averaging over species with common degree in the original community now gives

$$\begin{aligned} & \frac{1}{N_k^* N_{k'}^*} \sum_{i \in S_k^*} \sum_{j \in S_{k'}^*} \langle A_{ij} \theta_i^* \theta_j^* \rangle_{\mathbf{A}, \alpha} \\ &= \frac{1}{N_k^* N_{k'}^*} \sum_{i \in S_k^*} \sum_{j \in S_{k'}^*} \left\langle \frac{k_i k_j}{dN} \theta_i(t) \theta_j(t) \right\rangle_{\mathbf{A}, \alpha} = \frac{k k'}{dN}, \end{aligned} \quad (\text{E7})$$

as claimed in the main text.

The same method can be used to compute any statistics of the adjacency matrix in the surviving community. As we need it in the following section, we also have

$$\frac{1}{N_k^* N_{k'}^* N_{k''}^*} \sum_{i \in S_k^*} \sum_{j \in S_{k'}^*} \sum_{l \in S_{k''}^*} \langle A_{ij} A_{il} \theta_i^* \theta_j^* \theta_l^* \rangle_{\mathbf{A}, \alpha} = \frac{k^2 k' k''}{d^2 N^2}. \quad (\text{E8})$$

All higher moments of the adjacency matrix have similarly simple forms.

2. Degree sequence in the surviving community

Here we detail the derivation of the degree sequence in the surviving community. First, we will show that the expected degree of a species in the surviving community, given its degree in the original community, is given by Eq. (8) in the main text. We will then show that the degrees concentrate around their mean value.

To compute $E[k_i^* | k_i, i \in S^*]$, we write it in terms of the adjacency matrix in the surviving community. This gives [using Eq. (E7)]

$$\begin{aligned} E[k_i^* | k_i, i \in S^*] &= E \left[\sum_{j \in S^*} A_{ij}^* | k_i, i \in S^* \right] \\ &= \sum_{k'} N_{k'}^* \left(\frac{k_i k'}{dN} + O(d^0) \right) \\ &= k_i r + O(d^0), \end{aligned} \quad (\text{E9})$$

where we recall that $r = \sum_k p_k k \phi_k / \sum_k p_k k$ is the average neighbor survival rate in the community. The calculation of the variance proceeds in the same way: it relies on the additional calculation in Eq. (E8). We have

$$\begin{aligned} & E[(k_i^*)^2 | k_i, i \in S^*] - E[k_i^* | k_i, i \in S^*]^2 \\ &= E \left[\sum_{j, l \in S^*} A_{ij}^* A_{il}^* | k_i, i \in S^* \right] - E \left[\sum_{j \in S^*} A_{ij}^* | k_i, i \in S^* \right]^2 \\ &= \sum_{k, k'} N_k^* N_{k'}^* \frac{(k_i)^2 k k'}{d^2 N^2} - (k_i r)^2 + O(d^0) \\ &= O(d^0), \end{aligned} \quad (\text{E10})$$

as claimed in the main text.

3. Degree distribution in the surviving community

To leading order in $1/d$, the degrees of species in the surviving community concentrate around the mean value in Eq. (E9). Using this, we can find an expression for the degree distribution which is accurate to leading order in $1/d$ by simply approximating the degree sequence of a species in the surviving community with $k^* = kr$, where k is the degree of the species in the original community. As kr is not in general an integer, we will find an expression for the function $P^*(k^*/N) = N p_{k^*}^*$, which we assume is continuous for large N . The degree distribution in the original community can be written similarly as $P(k/N) = N p_k$. These expressions are normalized and satisfy

$$\begin{aligned} & \frac{1}{N} \sum_i f(k_i) = \sum_k p_k f(k) \approx \int_{\kappa_{\min}}^{\kappa_{\max}} P(\kappa) f(\kappa) d\kappa, \\ & \frac{1}{N^*} \sum_{i \in S^*} f(k_i^*) = \sum_{k^*} p_{k^*}^* f(k^*) \approx \int_{\kappa_{\min}^*}^{\kappa_{\max}^*} P^*(\kappa) f(\kappa) d\kappa, \end{aligned} \quad (\text{E11})$$

where $\kappa = k/N$ and $\kappa^* = k^*/N = r\kappa$. The approximations in Eq. (E11) hold for large N , which allows us to approximate the sums as integrals.

To find an expression for the degree distribution in the surviving community, we observe that the second of the expressions in Eqs. (E11) can also be computed as follows (using the approximation $k^* = kr$):

$$\begin{aligned} \frac{1}{N^*} \sum_{i \in S^*} f(k_i^*) &= \frac{1}{N^*} \sum_k N_k^* f(kr) \\ &= \frac{1}{\phi} \sum_k p_k \phi_k f(kr) \\ &= \frac{1}{\phi} \int_{\kappa_{\min}}^{\kappa_{\max}} d\kappa P(\kappa) \Phi(\kappa) f(\kappa r) \\ &= \frac{1}{\phi r} \int_{\kappa_{\min}^*}^{\kappa_{\max}^*} d\kappa P\left(\frac{\kappa}{r}\right) \Phi\left(\frac{\kappa}{r}\right) f(\kappa), \quad (\text{E12}) \end{aligned}$$

where $\Phi(k/N) = \phi_k$. The two expressions for $\frac{1}{N^*} \sum_{i \in S^*} f(k_i^*)$ in Eqs. (E11) and (E12) must be equal. As the function f is arbitrary, we conclude that the following equality holds:

$$P^*(\kappa) = \frac{1}{\phi r} P\left(\frac{\kappa}{r}\right) \Phi\left(\frac{\kappa}{r}\right), \quad (\text{E13})$$

which is Eq. (9) in the main text.

APPENDIX F: BARABÁSI-ALBERT NETWORKS

We further test our theory by applying it to a system for which the initial pool of species interacts on a Barabási-Albert network [72]. The use of a Chung-Lu network in our analysis is equivalent to an annealed network approximation [31,43], and thus applies to other networks. It is best suited to uncorrelated networks. In Barabási-Albert networks degrees are not strictly uncorrelated [73]. However, these correlations are known to be small (see, e.g., Ref. [74]), so the assumption of uncorrelated degrees is valid as an approximation.

Barabási-Albert networks can be constructed through a growth algorithm, adding a new node to an existing and using the well-known preferential attachment protocol to connect the new node to m existing nodes [72]. Asymptotically, this leads to a degree distribution of the form [53]

$$p_k = \frac{2m(m+1)}{k(k+1)(k+2)}. \quad (\text{F1})$$

The network is therefore scale-free, $p(k) \sim k^{-3}$ for large k .

In Figs. 8 and 9, we test our theory against simulations of communities for which the initial network is of the Barabási-Albert form. The theory appears to do quite well, despite the fact that it does not account for degree correlations.

APPENDIX G: SPECIFYING THE FINAL DEGREE DISTRIBUTION

In Sec. IV A, we determine the degree distribution in the surviving community, given the statistics of interactions and the degree distribution in the initial community. In this appendix, we address the inverse problem; i.e., we determine what initial communities give rise to surviving communities with a given degree distribution. Throughout this section, we write p_k for the discrete degree distribution in the initial community, and $P(\kappa)$ for a continuous function on $[0, 1]$ such

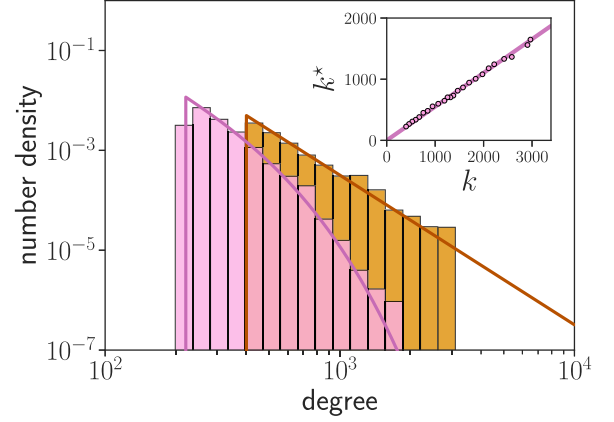


FIG. 8. Initial (orange straight) and final (pink curved) degree distributions in the case where the initial degree distribution is a Barabási-Albert network with $m = 400$ and $N = 10\,000$. Additional parameters are $\mu = -3.0$, $\sigma = 1.0$, $\gamma = 0.0$. Bars are the result of a single realization of the initial network and the final network resulting from the dynamics, respectively. Lines are from the theory with the Barabási-Albert degree distribution as input. The inset shows the degrees of species in the surviving community as a function of the degree in the original community. In the inset, only a subset of the points are shown to avoid overcrowding; no average is taken. The solid line in the inset is the line $k = rk^*$, where r is defined in the main text [see Eq. (8)].

that $P(k/N) = Np_k$. Similarly, we use p_{k^*} for the degree distribution in the surviving community and $P^*(k^*/N) = Np_{k^*}$, as well as ϕ_k for the survival rate of species with degree k and $\Phi(k/N) = \phi_k$. We also use $\kappa = k/N$ and $\kappa^* = k^*/N$.

We now outline the method in the case where the final degree distribution is scale-free, although it can be applied to any desired final degree distribution. Specifically, for given values of μ , σ , and γ , we find a degree distribution p_k in the initial community which produces a final degree distribution which is scale-free with exponent α :

$$p_{k^*}^* \propto (k^*)^{-\alpha}. \quad (\text{G1})$$

We use the following ansatz for the degree distribution in the original network,

$$p_k = A \frac{k^{-\alpha}}{\phi_k}, \quad (\text{G2})$$

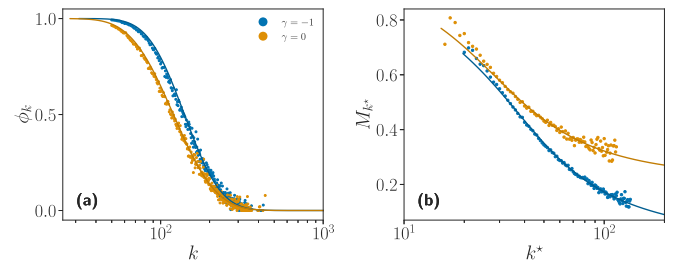


FIG. 9. Data similar to that in Fig. 5 of the main text, but for a Barabási-Albert network in the original community ($m = 50$, $N = 2000$). Parameters for the interaction strengths are $\mu = -3.0$, $\sigma = 1$, and values of γ are as indicated in (a). There is no curve for $\gamma = 1$ because the system is unstable for that choice of parameters.

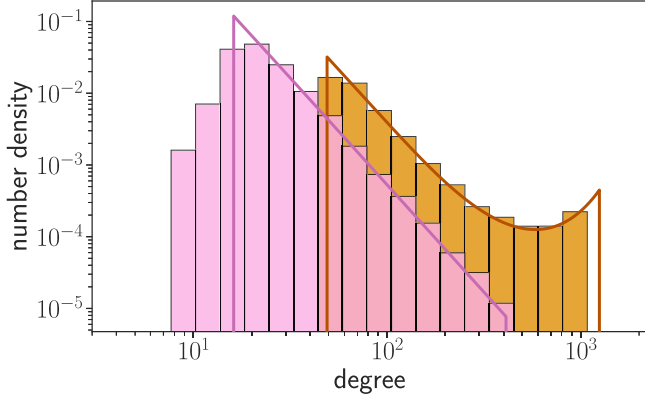


FIG. 10. Example of a degree distribution (orange bars on the right) which results in a scale-free final degree distribution (pink bars on the left). Statistics of the interactions are $\mu = -3.0$, $\sigma = 1.0$, $\gamma = 0.0$, and the final degree distribution is a power law with exponent 3. Bars are from a single run of the dynamics with $N = 10000$ species in the initial community. To mitigate issues with constructing networks with the required degree distributions, we have imposed a minimum and a maximum degree for the degree distribution in the initial community (see, e.g., Ref. [75]). The occurrence of more low-degree species in the final network than expected from the theory is likely due to a combination of finite-size effects and network sparsity, both of which our theory does not take into account.

where A is a normalization constant ensuring $\sum_k p_k = 1$. As the survival rates ϕ_k depend on the degree distribution p_k in the initial community, they must be determined self-consistently. If there are survival rates which satisfy this self-consistent requirement, then application of Eq. (9) from the main text reveals that the final degree distribution is scale-free, as required:

$$P^*(\kappa^*) = \frac{A}{\phi r} \frac{\Phi(\frac{\kappa^*}{r}) (\frac{\kappa^*}{r})^{-\alpha}}{\Phi(\frac{\kappa^*}{r})} \propto (\kappa^*)^{-\alpha}, \quad (\text{G3})$$

or, in discrete form, $p_{k^*}^* \propto (k^*)^{-\alpha}$.

To determine the survival rates $\{\phi_k\}$, we insert the degree distribution p_k from Eq. (G2) into the fixed-point equations [see Eqs. (A23)]. This gives

$$\begin{aligned} \chi_k &= w_0(\Delta_k) \left[1 - \frac{A\gamma\sigma^2 k}{d^2} \sum_{k'} \frac{(k')^{-\alpha}}{w_0(\Delta_{k'})} k' \chi_{k'} \right]^{-1}, \\ M_k &= w_1(\Delta_k) \Sigma_k, \\ q_k &= w_2(\Delta_k) \Sigma_k^2, \end{aligned} \quad (\text{G4})$$

where

$$\begin{aligned} \Sigma_k &= \sqrt{\frac{A\sigma^2 k}{d^2} \sum_{k'} \frac{(k')^{-\alpha}}{w_0(\Delta_{k'})} k' q_{k'}} \\ &\times \left[1 - \frac{A\gamma\sigma^2 k}{d^2} \sum_{k'} \frac{(k')^{-\alpha}}{w_0(\Delta_{k'})} k' \chi_{k'} \right]^{-1}, \end{aligned}$$

$$\begin{aligned} \Delta_k &= \left[1 + \frac{A\mu k}{d^2} \sum_{k'} \frac{(k')^{-\alpha}}{w_0(\Delta_{k'})} k' M_{k'} \right] \\ &\times \left[\sqrt{\frac{A\sigma^2 k}{d^2} \sum_{k'} \frac{(k')^{-\alpha}}{w_0(\Delta_{k'})} k' q_{k'}} \right]^{-1}, \end{aligned} \quad (\text{G5})$$

and where we have used $w_0(\Delta_k) = \phi_k$. The (initial) degree distribution is unknown in these equations. We must add two further constraints to ensure that p_k is normalized and that d is the average degree in the initial network:

$$\begin{aligned} A \sum_k \frac{k^{-\alpha}}{w_0(\Delta_k)} k &= d, \\ A \sum_k \frac{k^{-\alpha}}{w_0(\Delta_k)} &= 1. \end{aligned} \quad (\text{G6})$$

Equations (G4), together with Eqs. (G6), define a system of at most $3k_{\max} + 2$ equations in the unknowns M_k , q_k , χ_k , d , and A . Similarly to Appendix A 1, we can write the self-consistent equations in a more convenient form by defining the following parameters:

$$\begin{aligned} U &= \frac{A\mu}{d^2} \sum_{k'} \frac{(k')^{-\alpha}}{w_0(\Delta_{k'})} k' M_{k'}, \\ S^2 &= \frac{A\sigma^2}{d^2} \sum_{k'} \frac{(k')^{-\alpha}}{w_0(\Delta_{k'})} k' q_{k'}, \\ T &= \frac{A\gamma\sigma^2}{d^2} \sum_{k'} \frac{(k')^{-\alpha}}{w_0(\Delta_{k'})} k' \chi_{k'}. \end{aligned} \quad (\text{G7})$$

In terms of these quantities, our self-consistent equations are

$$\begin{aligned} U &= \frac{AS\mu}{d^2} \sum_k \frac{k^{-\alpha} k^{\frac{3}{2}}}{1 - Tk} \frac{w_1\left(\frac{1+Uk}{S\sqrt{k}}\right)}{w_0\left(\frac{1+Uk}{S\sqrt{k}}\right)}, \\ 1 &= \frac{A\sigma^2}{d^2} \sum_k \frac{k^{-\alpha} k^2}{(1 - Tk)^2} \frac{w_2\left(\frac{1+Uk}{S\sqrt{k}}\right)}{w_0\left(\frac{1+Uk}{S\sqrt{k}}\right)}, \\ T &= \frac{A\gamma\sigma^2}{d^2} \sum_k \frac{k^{-\alpha} k}{(1 - Tk)}, \\ d &= A \sum_k \frac{k^{-\alpha} k}{w_0\left(\frac{1+Uk}{S\sqrt{k}}\right)}, \\ A &= \left(\sum_k \frac{k^{-\alpha}}{w_0\left(\frac{1+Uk}{S\sqrt{k}}\right)} \right)^{-1}. \end{aligned} \quad (\text{G8})$$

To summarize: For given μ, σ, γ , and α , the following steps will produce a surviving community whose network of

interactions has a scale-free degree distribution with exponent α . First, solve Eqs. (G8) for the unknowns A , d , U , S , and T . Then, run the dynamics on a community with interaction statistics μ , σ , γ and degree distribution

$$p_k = A \frac{k^{-\alpha}}{w_0 \left(\frac{1+Uk}{S\sqrt{k}} \right)}. \quad (\text{G9})$$

The degree distribution in the resulting surviving community will be scale-free with exponent α . Figure 10 demonstrates that it is possible to solve Eqs. (G8) in the case where $\alpha = 3$. We emphasize that while we have shown the procedure in the case of a scale-free network, this can be generalized to other shapes of the desired degree distribution among surviving species.

-
- [1] J. Grilli, Macroecological laws describe variation and diversity in microbial communities, *Nat. Commun.* **11**, 4743 (2020).
 - [2] W. R. Shoemaker, Á. Sánchez, and J. Grilli, Macroecological patterns in experimental microbial communities, bioRxiv, doi:10.1101/2023.07.24.550281.
 - [3] J. H. Brown, *Macroecology* (University of Chicago Press, Chicago, 1995).
 - [4] S. Xu, L. Böttcher, and T. Chou, Diversity in biology: Definitions, quantification and models, *Phys. Biol.* **17**, 031001 (2020).
 - [5] X. Liu, G. W. A. Constable, and J. W. Pitchford, Feasibility and stability in large Lotka Volterra systems with interaction structure, *Phys. Rev. E* **107**, 054301 (2023).
 - [6] M. Pascual and J. A. Dunne, *Ecological Networks: Linking Structure to Dynamics in Food Webs* (Oxford University Press, New York, 2006).
 - [7] J. Bascompte, P. Jordano, C. J. Melián, and J. M. Olesen, The nested assembly of plant–animal mutualistic networks, *Proc. Natl. Acad. Sci. USA* **100**, 9383 (2003).
 - [8] E. Sebastián-González, B. Dalsgaard, B. Sandel, and P. R. Guimarães, Jr., Macroecological trends in nestedness and modularity of seed-dispersal networks: Human impact matters, *Global Ecol. Biogeogr.* **24**, 293 (2015).
 - [9] U. Bastolla, M. A. Fortuna, A. Pascual-García, A. Ferrera, B. Luque, and J. Bascompte, The architecture of mutualistic networks minimizes competition and increases biodiversity, *Nature (London)* **458**, 1018 (2009).
 - [10] U. Bastolla, M. Lässig, S. C. Manrubia, and A. Valleriani, Biodiversity in model ecosystems, I: Coexistence conditions for competing species, *arXiv:q-bio/0502021*.
 - [11] J. A. Dunne, R. J. Williams, and N. D. Martinez, Food-web structure and network theory: The role of connectance and size, *Proc. Natl. Acad. Sci. USA* **99**, 12917 (2002).
 - [12] A.-M. Neutel, J. A. P. Heesterbeek, and P. C. de Ruiter, Stability in real food webs: Weak links in long loops, *Science* **296**, 1120 (2002).
 - [13] M. Lurgi, D. Montoya, and J. M. Montoya, The effects of space and diversity of interaction types on the stability of complex ecological networks, *Theor. Ecol.* **9**, 3 (2016).
 - [14] P. Landi, H. O. Minoarivelo, Å. Brännström, C. Hui, and U. Dieckmann, Complexity and stability of ecological networks: A review of the theory, *Popul. Ecol.* **60**, 319 (2018).
 - [15] R. P. Rohr, S. Saavedra, and J. Bascompte, On the structural stability of mutualistic systems, *Science* **345**, 1253497 (2014).
 - [16] J. A. Fuhrman, Microbial community structure and its functional implications, *Nature (London)* **459**, 193 (2009).
 - [17] R. M. Thompson, U. Brose, J. A. Dunne, R. O. Hall, S. Hladysz, R. L. Kitching, N. D. Martinez, H. Rantala, T. N. Romanuk, D. B. Stouffer, and J. M. Tylianakis, Food webs: Reconciling the structure and function of biodiversity, *Trends Ecol. Evol.* **27**, 689 (2012).
 - [18] K. Faust and J. Raes, Microbial interactions: From networks to models, *Nat. Rev. Microbiol.* **10**, 538 (2012).
 - [19] E. W. Jones and J. M. Carlson, Steady-state reduction of generalized Lotka-Volterra systems in the microbiome, *Phys. Rev. E* **99**, 032403 (2019).
 - [20] J. E. Cohen, 13. Food webs and community structure, in *Perspectives in Ecological Theory*, edited by J. Roughgarden, R. M. May, and S. A. Levin (Princeton University Press, Princeton, NJ, 1989), pp. 181–202.
 - [21] J. E. Cohen, A stochastic theory of community food webs. VI. Heterogeneous alternatives to the cascade model, *Theor. Popul. Biol.* **37**, 55 (1990).
 - [22] J. E. Cohen, F. Briand, C. M. Newman, and J. H. Steele, A stochastic theory of community food webs. III. Predicted and observed lengths of food chains, *Proc. R. Soc. London B* **228**, 317 (1997).
 - [23] R. J. Williams and N. D. Martinez, Simple rules yield complex food webs, *Nature (London)* **404**, 180 (2000).
 - [24] R. J. Williams and N. D. Martinez, Stabilization of chaotic and non-permanent food-web dynamics, *Eur. Phys. J. B* **38**, 297 (2004).
 - [25] S. Allesina, D. Alonso, and M. Pascual, A general model for food web structure, *Science* **320**, 658 (2008).
 - [26] S. Allesina, J. Grilli, G. Barabás, S. Tang, J. Aljadeff, and A. Maritan, Predicting the stability of large structured food webs, *Nat. Commun.* **6**, 7842 (2015).
 - [27] R. M. May, Will a large complex system be stable? *Nature (London)* **238**, 413 (1972).
 - [28] G. Barabás, M. J. Michalska-Smith, and S. Allesina, The effect of intra- and interspecific competition on coexistence in multi-species communities, *Am. Nat.* **188**, E1 (2016).
 - [29] J. Grilli, T. Rogers, and S. Allesina, Modularity and stability in ecological communities, *Nat. Commun.* **7**, 12031 (2016).
 - [30] L. Poley, T. Galla, and J. W. Baron, Eigenvalue spectra of finely structured random matrices, *arXiv:2311.02006*.
 - [31] J. W. Baron, Eigenvalue spectra and stability of directed complex networks, *Phys. Rev. E* **106**, 064302 (2022).
 - [32] T. Galla, Dynamically evolved community size and stability of random Lotka-Volterra ecosystems, *EPL (Europhys. Lett.)* **123**, 48004 (2018).
 - [33] G. Bunin, Ecological communities with Lotka-Volterra dynamics, *Phys. Rev. E* **95**, 042414 (2017).
 - [34] M. Barbier, C. de Mazancourt, M. Loreau, and G. Bunin, Fingerprints of high-dimensional coexistence in complex ecosystems, *Phys. Rev. X* **11**, 011009 (2021).

- [35] M. Barbier, J. Arnoldi, G. Bunin, and M. Loreau, Generic assembly patterns in complex ecological communities, *Proc. Natl. Acad. Sci. USA* **115**, 2156 (2018).
- [36] G. Bunin, Interaction patterns and diversity in assembled ecological communities, [arXiv:1607.04734](https://arxiv.org/abs/1607.04734).
- [37] J. W. Baron, T. J. Jewell, C. Ryder, and T. Galla, Breakdown of random-matrix universality in persistent Lotka-Volterra communities, *Phys. Rev. Lett.* **130**, 137401 (2023).
- [38] F. Aguirre-López, Heterogeneous mean-field analysis of the generalized Lotka–Volterra model on a network, *J. Phys. A: Math. Theor.* **57**, 345002 (2024).
- [39] J. I. Park, D.-S. Lee, S. H. Lee, and H. J. Park, Incorporating heterogeneous interactions for ecological biodiversity, *Phys. Rev. Lett.* **133**, 198402 (2024).
- [40] B. Bollobás, A probabilistic proof of an asymptotic formula for the number of labelled regular graphs, *Eur. J. Combinatorics* **1**, 311 (1980).
- [41] M. Newman, *Networks* (Oxford University Press, Oxford, 2018).
- [42] F. Chung and L. Lu, Connected components in random graphs with given expected degree sequences, *Ann. Combinatorics* **6**, 125 (2002).
- [43] A. Carro, R. Toral, and M. San Miguel, The noisy voter model on complex networks, *Sci. Rep.* **6**, 24775 (2016).
- [44] L. Poley, J. W. Baron, and T. Galla, Generalized Lotka-Volterra model with hierarchical interactions, *Phys. Rev. E* **107**, 024313 (2023).
- [45] A. Altieri, F. Roy, C. Cammarota, and G. Biroli, Properties of equilibria and glassy phases of the random Lotka-Volterra model with demographic noise, *Phys. Rev. Lett.* **126**, 258301 (2021).
- [46] E. Mallmin, A. Traulsen, and S. De Monte, Chaotic turnover of rare and abundant species in a strongly interacting model community, *Proc. Natl. Acad. Sci. USA* **121**, e2312822121 (2024).
- [47] G. Garcia Lorenzana and A. Altieri, Well-mixed Lotka-Volterra model with random strongly competitive interactions, *Phys. Rev. E* **105**, 024307 (2022).
- [48] M. Mézard, G. Parisi, and M. Virasoro, *Spin Glass Theory and Beyond: An Introduction to the Replica Method and Its Applications* (World Scientific, London, 1987), Vol. 9.
- [49] C. De Dominicis, Dynamics as a substitute for replicas in systems with quenched random impurities, *Phys. Rev. B* **18**, 4913 (1978).
- [50] H. Janssen, On a Lagrangean for classical field dynamics and renormalization group calculations of dynamical critical properties, *Z. Phys. B* **23**, 377 (1976).
- [51] P. C. Martin, E. D. Siggia, and H. A. Rose, Statistical dynamics of classical systems, *Phys. Rev. A* **8**, 423 (1973).
- [52] M. Oppen and S. Diederich, Phase transition and $1/f$ noise in a game dynamical model, *Phys. Rev. Lett.* **69**, 1616 (1992).
- [53] S. N. Dorogovtsev, J. F. F. Mendes, and A. N. Samukhin, Structure of growing networks with preferential linking, *Phys. Rev. Lett.* **85**, 4633 (2000).
- [54] E. L. Sander, J. T. Wootton, and S. Allesina, Ecological network inference from long-term presence-absence data, *Sci. Rep.* **7**, 17154 (2017).
- [55] D. S. Maynard, J. T. Wootton, C. A. Serván, and S. Allesina, Reconciling empirical interactions and species coexistence, *Ecol. Lett.* **22**, 1028 (2019).
- [56] P. L. Nguyen, F. Pomati, and R. P. Rohr, Inferring intrinsic population growth rates and per capita interactions from ecological time-series, [bioRxiv](https://arxiv.org/abs/2404.11111) (2024).
- [57] J. Camacho, R. Guimera, and L. A. Nunes Amaral, Analytical solution of a model for complex food webs, *Phys. Rev. E* **65**, 030901 (2002).
- [58] J. Camacho, R. Guimerà, and L. A. Nunes Amaral, Robust patterns in food web structure, *Phys. Rev. Lett.* **88**, 228102 (2002).
- [59] C. A. Serván, J. A. Capitán, J. Grilli, K. E. Morrison, and S. Allesina, Coexistence of many species in random ecosystems, *Nat. Ecol. Evol.* **2**, 1237 (2018).
- [60] R. Milo, S. Shen-Orr, S. Itzkovitz, N. Kashtan, D. Chklovskii, and U. Alon, Network motifs: Simple building blocks of complex networks, *Science* **298**, 824 (2002).
- [61] L. Stone, D. Simberloff, and Y. Artzy-Randrup, Network motifs and their origins, *PLoS Comput. Biol.* **15**, e1006749 (2019).
- [62] D. B. Stouffer, J. Camacho, R. Guimerà, C. A. Ng, and L. A. Nunes Amaral, Quantitative patterns in the structure of model and empirical food webs, *Ecology* **86**, 1301 (2005).
- [63] D. B. Stouffer, J. Camacho, and L. A. N. Amaral, A robust measure of food web intervality, *Proc. Natl. Acad. Sci. USA* **103**, 19015 (2006).
- [64] C. J. Melián and J. Bascompte, Food web structure and habitat loss, *Ecol. Lett.* **5**, 37 (2002).
- [65] D. Garlaschelli and M. I. Loffredo, Patterns of link reciprocity in directed networks, *Phys. Rev. Lett.* **93**, 268701 (2004).
- [66] D. Garlaschelli, G. Caldarelli, and L. Pietronero, Universal scaling relations in food webs, *Nature (London)* **423**, 165 (2003).
- [67] J. W. Baron, A path integral approach to sparse non-Hermitian random matrices, [arXiv:2308.13605](https://arxiv.org/abs/2308.13605).
- [68] C. De Dominicis and L. Peliti, Field-theory renormalization and critical dynamics above T_c : Helium, antiferromagnets, and liquid-gas systems, *Phys. Rev. B* **18**, 353 (1978).
- [69] S. Azaele and A. Maritan, Large system population dynamics with non-Gaussian interactions, [arXiv:2306.13449](https://arxiv.org/abs/2306.13449).
- [70] J. E. Cohen, Derivatives of the spectral radius as a function of non-negative matrix elements, *Math. Proc. Cambridge Philos. Soc.* **83**, 183 (1978).
- [71] E. Deutsch and M. Neumann, Derivatives of the Perron root at an essentially nonnegative matrix and the group inverse of an M-matrix, *J. Math. Anal. Appl.* **102**, 1 (1984).
- [72] R. Albert and A.-L. Barabási, Statistical mechanics of complex networks, *Rev. Mod. Phys.* **74**, 47 (2002).
- [73] B. Fotouhi and M. G. Rabbat, Degree correlation in scale-free graphs, *Eur. Phys. J. B* **86**, 510 (2013).
- [74] V. Sood and S. Redner, Voter model on heterogeneous graphs, *Phys. Rev. Lett.* **94**, 178701 (2005).
- [75] D. Fasino, A. Tonetto, and F. Tudisco, Generating large scale-free networks with the Chung-Lu random graph model, [arXiv:1910.11341](https://arxiv.org/abs/1910.11341).